# “Effect of silver nanoparticles on properties and performance of aquaporin forward osmosis membrane”

**Amire Anuarbek**, B.Eng


**School of Engineering**

**Department of Civil and Environmental Engineering**

**Nazarbayev University**

53, Kabanbay Batyr Avenue,

Astana, Kazakhstan, 010000

**Supervisor:** Elizabeth Arkhangelsky, Associate Professor

**January 2019**

DECLARATION

I hereby, declare that this manuscript, entitled *"Effect of silver nanoparticles on properties and performance of aquaporin forward osmosis membrane",* is the result of my own work except for quotations and citations which have been duly acknowledged.

I also declare that, to the best of my knowledge and belief, it has not been previously or concurrently submitted, in whole or in part, for any other degree or diploma at Nazarbayev University or any other national or international institution.

Name:

Date:

# Abstract

Due to the scarcity of clean water in many regions of the world, seawater desalination and wastewater treatment start to play a crucial role for future water supplies. Currently leading technology of membrane water treatment is based on conventional technologies (reverse osmosis, nanofiltration, ultrafiltration and microfiltration) consuming high amount of energy. One of the ways to solve the problems with overconsumption of energy is to use forward osmosis (FO). FO is a relatively new membrane-based process that can significantly upgrade water treatment technologies. Since it employs membrane technology, the performance of the forward osmosis water treatment directly depends on properties of the membrane whose performance highly vulnerable to fouling activities.

One of the ways to increase membrane performance is to use aquaporin-biological protein that forms selective natural water channels that facilitate water permeation when integrated into a membrane. Aquaporin membranes have received increasing attention because of their high water permeability and superior selectivity. However, the usage of aquaporin membranes as a selectively permeable material has its risks of accumulation of small biological organisms and organic compounds that impede functionality of membrane. Thus, there is a need

for biological and organic fouling mitigation for the production of optimized membrane.

This study proposes aquaporin membranes coupled with silver nanoparticles (Ag-NPs) that are known as highly efficient biocidal materials. Also, silver nanoparticles are revealed to be efficient against organic macromolecules that can result from secretion of extracellular polymeric substances (EPS). To understand how addition of Ag-NPs influence on properties and performance of water filtration membranes, original aquaporin based membrane is experimentally examined. Then, membranes modified with nanoparticles is tested and compared with original membrane. In this study two hypotheses were suggested: Whether silver nanoparticles inhibit the functionality of aquaporins; if no, whether silver nanoparticles are able to decrease organic compounds and resulting biofouling, which cause significant damage to membrane treatment processes.

Method of the modification consisted of several parts, which included synthesis of silver nanoparticles based on the procedure suggested by Geuze and Slot, and the process of modification of the membrane itself. Performance assessment was conducted by observing effect of Ag-NPs on baseline experiments and post-cleaning water flux change. Results of conducted experiments demonstrate that aquaporin membrane was successfully modified with silver nanoparticles. Silver nanoparticles improved the qualities and functions of

aquaporin membrane, which resulted in optimization of water treatment process. Moreover, modification of aquaporin membrane with silver nanoparticles improves antibacterial properties of membrane.

**Keywords**: forward osmosis, aquaporin, silver nanoparticles, biofouling, organic fouling, FTIR, zeta potential, SEM, flux loss, cleaning.

# Acknowledgements

Over the last year I have experienced things that contributed a lot to my personal and academic development. This work is the result of the hard work that me and my supervisor Elizabeth Arkhangelsky have done through everyday experiments, analysis and discussion of possible implications. With sincere acknowledgement, I want to thank my supervisor Elizabeth Arkhangelsky for her support and lessons that she taught me. Thanks to the time that we have worked together I understood the importance of proactivity, lifelong learning and natural interest in what you are doing.

I also want to thank those people who also contributed to the development of this study and made it possible. I want to thank Nazarbayev University School of Engineering for providing necessary materials and equipment needed for my experiments; my professors from the department of Civil Engineering for helping me to keep and save my academic interest, my group mates who were always there for me ready to help, and Aliya Satayeva for helping me with all the things in laboratory. This kind of support from members of our scientific community is crucial, and can be considered as an essential for young engineers. I also want to thank Samat (from SST, biology department) for helping with disk experiments, and Rakhima Shamenova (from NLA) for giving access to SEM.

I want to give my sincere thanks to my family. Dearest dad, mom, Aito, Aigera and Aida, you are the most valuable people in the world for me, and I will never stop thanking you for being supportive, kind, critical where needed and loving all the time. The level of emotional support that you provided me with guided me with the light in my darkest times, and I know that I will never stop seeing this light. All of you made this possible.

# Table of Contents


Abstract ..... 3
Acknowledgements ..... 6
Table of Contents ..... 8
List of figures ..... 10
List of tables ..... 13
List of Abbreviations ..... 14
Chapter 1 – Introduction ..... 1
1.1. Water problem ..... 1
1.2. Membrane processes ..... 1
1.3. Classification of conventional membranes ..... 4
1.4. Forward osmosis ..... 10
1.5. Aquaporin incorporation ..... 12
1.6. Fouling ..... 14
1.7. Concentration polarization ..... 18
1.8. Fouling mitigation by silver nanoparticles ..... 19
1.9. Research significance and objectives ..... 21
Chapter 2 – Materials and methods ..... 23
2.1 – Materials ..... 23
2.2 – Modification methods ..... 24
2.2.1 – Synthesis of silver nanoparticles ..... 24
2.2.2 – Attachment of Ag-NPs ..... 24
2.3 – Chemical and morphological characterization ..... 25
2.3.1 – Size and zeta potential of silver nanoparticles ..... 25
2.3.2 – Zeta potential of membrane ..... 26
2.3.3 – FTIR ..... 26
2.3.4 – Optical microscope ..... 27

2.3.5 – SEM/EDX ..... 27
2.3.6 – Contact angle ..... 27
2.3.7 – XRF/XRD ..... 28
2.4 – Baseline and Fouling experiments ..... 28
2.4.1 – Effect of Ag-NPs on performance of aquaporin channels ..... 30
2.4.2 – Effect of Ag-NPs on cleaning of membranes ..... 32
2.5 – Antimicrobial properties of modified membrane ..... 33
Chapter 3 – Results and Discussion ..... 34
3.1 – Characterization of Ag-NPs ..... 34
3.1.1 – Size of AgNPs ..... 34
3.1.2 – Zeta potential of AgNPs ..... 35
3.2 – Characterization of pristine and modified membranes ..... 37
3.2.1 – FTIR ..... 37
3.2.2 – Zeta potential ..... 41
3.2.3 – Optical microscopy ..... 45
3.2.4 – Contact angle ..... 46
3.2.5 – SEM/EDX ..... 48
3.2.6 – XRF and XRD ..... 52
3.3 – Antimicrobial properties of membrane ..... 55
3.4 – Effect of Ag-NPs on performance of aquaporin channels ..... 57
3.5 – Effect of Ag-NPs on cleaning of membranes ..... 60
3.5.1 – Surface rinsing ..... 61
3.5.2 – Osmotic backwash ..... 65
3.5.3 – CFV magnification ..... 68
Chapter 4 – Conclusion ..... 72
References ..... 74

# List of figures

Figure 1-1. Graphical representation of general filtration process ..... 3
Figure 1-2. Diagram of (a) cross-flow filtration and (b) dead-end filtration ..... 4
Figure 1-3. General structure of thin film composite membrane ..... 5
Figure 1-4. Ranges of applications of conventional membrane technologies [10] ... 7
Figure 1-5. Water flows of forward osmosis and reverse osmosis ..... 10
Figure 1-6. Schematic representation of the bacterial biofilm formation on an impermeable surface [30] ..... 17
Figure 1-7. Illustration of ICP through asymmetric FO membrane in active layer facing feed solution ..... 19
Figure 2-1. Covalently binding of silver nanoparticles to TFC membrane [48] .... 25
Figure 2-2. Schematic representation of FO lab scale setup ..... 29
Figure 3-1. Size of Ag-NPs as a function of pH ..... 34
Figure 3-2. Zeta potential of Ag-NPs as a function of pH ..... 35
Figure 3-3. FTIR spectrum of active layer of pristine FO membrane ..... 37
Figure 3-4. Chemical structure of a typical polyamide used as the surface layer TFC FO membrane [62] ..... 39
Figure 3-5. FTIR spectra of active layer of pristine and modified TFC FO membrane ..... 40
Figure 3-6. Zeta potential of pristine membrane for 1mM KCl electrolyte solution as a function of pH ..... 41
Figure 3-7. Zeta potential of pristine and modified membranes for 1mM KCl electrolyte solution ..... 43
Figure 3-8. Optical microscope images of active layer of pristine FO membrane under a) x400 magnification and b) x1000 magnification ..... 45
Figure 3-9. Optical microscope images of active layer of modified FO membrane under x1000 magnification a) focusing on a surface and b) focusing on pores ..... 46
Figure 3-10. Contact angle measurement of active layer for pristine and modified membranes ..... 46
Figure 3-11. SEM image of PA layer of pristine TFC FO membrane under x50k magnification ..... 47
Figure 3-12. EDX spectrum of pristine TFC FO membrane ..... 48
Figure 3-13. SEM image of polyamide layer of modified TFC FO membrane ..... 50

Figure 3-14. EDX spectra of modified TFC FO membrane ..... 51
Figure 3-15. XRF results of active layer of pristine TFC FO membrane ..... 52
Figure 3-16. XRD results of active layer of pristine TFC FO membrane ..... 53
Figure 3-17. XRF results of active layer of modified TFC FO membrane..... 53
Figure 3-18. XRD results of active layer of modified TFC FO membrane ..... 55
Figure 3-19. (a) Disk experiments before removing membrane samples. (b) Disk experiments after removing membrane samples. Incubation duration – 24 hours. E.coli bacteria in LB agar broth. ..... 56
Figure 3-20. . Low flux levels FO baseline experiments for pristine and modified membranes. AL-FS orientation at 12 m/s CFV in a cross flow mode. Feed 10 mM NaCl, draw pre-adjusted NaCl solution. ..... 58
Figure 3-21. High flux levels FO baseline experiments for pristine and modified membranes. AL-FS orientation at 12 cm/s CFV in a cross flow mode. Feed 10 mM NaCl, draw pre-adjusted NaCl solution. ..... 59
Figure 3-22. FO baseline experiments for pristine membrane. AL-FS orientation at 1.5 m/s CFV in a cross flow mode. Feed 10 mM NaCl, draw pre-adjusted NaCl solution. ..... 61
Figure 3-23. Normalized water flux of fouling experiment for pristine membrane: a) before surface rinsing and b) after surface rinsing. Experimental conditions for fouling experiments: feed solution (mixture of ALG (100 ppm), BSA (100 ppm) and TA (100 ppm), $CaCl_2$ (10 mM) and NaCl (10 mM); draw solution (5 M NaCl); AL-FS orientation; 1.5 cm/s CFV ..... 62
Figure 3-24. Normalized water flux of fouling experiment for modified membrane: a) before surface rinsing and b) after surface rinsing. Experimental conditions for fouling experiments: feed solution (mixture of ALG (100 ppm), BSA (100 ppm) and TA (100 ppm), $CaCl_2$ (10 mM) and NaCl (10 mM); draw solution (5 M NaCl); AL-FS orientation; 1.5 cm/s CFV ..... 64
Figure 3-25. Normalized water flux of fouling experiment for pristine membrane: a) before osmotic backwash and b) after osmotic backwash. Experimental conditions for fouling experiments: feed solution (mixture of ALG (100 ppm), BSA (100 ppm) and TA (100 ppm), $CaCl_2$ (10 mM) and NaCl (10 mM); draw solution (5 M NaCl); AL-FS orientation; 1.5 cm/s CFV ..... 65
Figure 3-26. Normalized water flux of fouling experiment for modified membrane: a) before osmotic backwash and b) after osmotic backwash. Experimental conditions for fouling experiments: feed solution (mixture of ALG (100 ppm), BSA (100 ppm) and TA (100 ppm), $CaCl_2$ (10 mM) and NaCl (10 mM); draw solution (5 M NaCl); AL-FS orientation; 1.5 cm/s ..... 67

Figure 3-27. Normalized water flux of fouling experiment for pristine membrane: a) before CFV magnification and b) CFV magnification. Experimental conditions for fouling experiments: feed solution (mixture of ALG (100 ppm), BSA (100 ppm) and TA (100 ppm), $CaCl_2$ (10 mM) and NaCl (10 mM); draw solution (5 M NaCl); AL-FS orientation; 1.5 cm/s CFV for the 1st run, 6 cm/s CFV for the 2nd run ..... 68
Figure 3-28. Normalized water flux of fouling experiment for modified membrane: a) before CFV magnification and b) CFV magnification. Experimental conditions for fouling experiments: feed solution (mixture of ALG (100 ppm), BSA (100 ppm) and TA (100 ppm), $CaCl_2$ (10 mM) and NaCl (10 mM); draw solution (5 M NaCl); AL-FS orientation; 1.5 cm/s CFV for the 1st run, 6 cm/s CFV for the 2nd run ..... 69

# List of tables

Table 3-1. Functional groups of polyamide and stretchings on FTIR spectra..... 38

# List of Abbreviations

| | |
|---|---|
| Ag-NP | silver nanoparticles |
| ALG | alginate |
| ATP | adenosine triphosphate |
| BSA | bovine serum albumin |
| CA | cellulose acetate |
| CFV | cross flow velocity |
| EDX | energy-dispersive X-ray spectroscopy |
| EPS | extracellular polymeric substance |
| FO | forward osmosis |
| FTIR | Fourier-transform infrared spectroscopy |
| LMH | L/m2/hr |
| MF | microfiltration |
| NF | nanofiltration |
| PA | polyamide |
| PES | polyether sulfone |
| PSF | polysulfone |
| RO | reverse osmoisis |
| SEM | scanning electron microscopy |
| TA | tannic acid |
| TFC | thin film composite |
| UF | ultrafiltration |
| WHO | World Health Organistaion |
| XRD | X-ray diffraction |
| XRF | X-ray fluorescence |

# Chapter 1 – Introduction

## 1.1. Water problem

Throughout history of human being clean water was an irreplaceable part of daily life. It always been demanded for such vital purposes as agriculture, industry and household use. As a result of the world population growth, need for energy conservation, improper water management, climate change and high potential for future water need, water challenge has become global issue that need to be addressed [1]. According to the statistics provided by United Nations, 1.2 billion people lack access to fresh drinking water and 1.7 billion people live in areas with insufficient water infrastructure [2]. According to the World Health Organization (WHO), poor water quality has lead to death of 3.4 million people each year caused by water related infections [3]. In addition to this, agriculture sector also suffers from lack of improved water which leads to decrease of food supply and famine in some regions of the globe [1]. Thus, it is seen that the effect of poor fresh water supply requires action to address current problem thus to improve treatment technology.

## 1.2. Membrane processes

Membrane technology is used in wide spectrum of applications in water industry to produce high quality water for different purposes. Membrane separation

technologies considered as the emerging water treatment technology among conventional water treatment technologies such as disinfection, distillation and media filtration. This owes to the fact that membrane technologies unlike processes above do not require chemical additives, heating and therefore use less energy [4]. What is more, from aspect of energy efficiency membrane technology is good solution in terms of sustainability and energy savings [4].

Looking at the history of the use of membranes in industry, one can find that, despite the fact that it was used in science since the mid-18th century, it became more widely used for desalination in the 1970s [5]. Over time, the capabilities of the membrane were further explored, and the new features discovered were used for broader purposes. Starting from the 21st century, the use of membrane separation processes for industrial purposes has attracted increasing attention of industry as well as academia [1].

In general, membrane plays a key role in water treatment processes and it is defined as selective barrier that allows some constituents to pass through and others to hold, in other words to separate permeate from feed stream (Figure 1-1) [4].

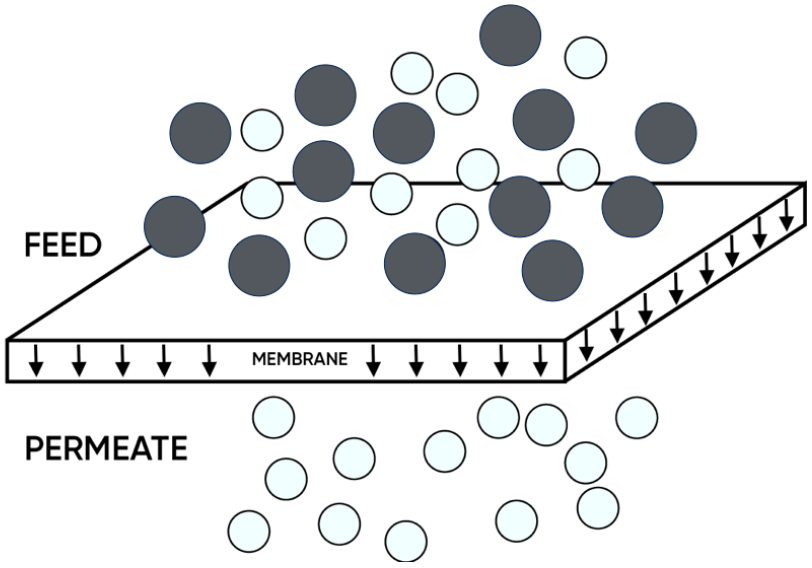


***Figure 1-1. Graphical representation of general filtration process***

The diluted solution that passes through the membrane is known as permeate, and the remaining concentrated solution is defined as retentate or brine [5]. Driving force for movement of permeate through membrane can vary from pressure difference, concentration difference, temperature difference or electric potential difference based on processes applied for water treatment [5]. Depending on the properties of the membrane and the properties of the dissolved particles, the permeability and the lifespan of the membrane are controlled.

Depending on the configurations operated, the membrane process is divided into dead-end filtration and cross-flow filtration. The process in which the input solution (feed) moves parallel to the surface of the membrane and two streams are formed (retentate and permeate) is known as cross-flow filtration (Figure 1-2).

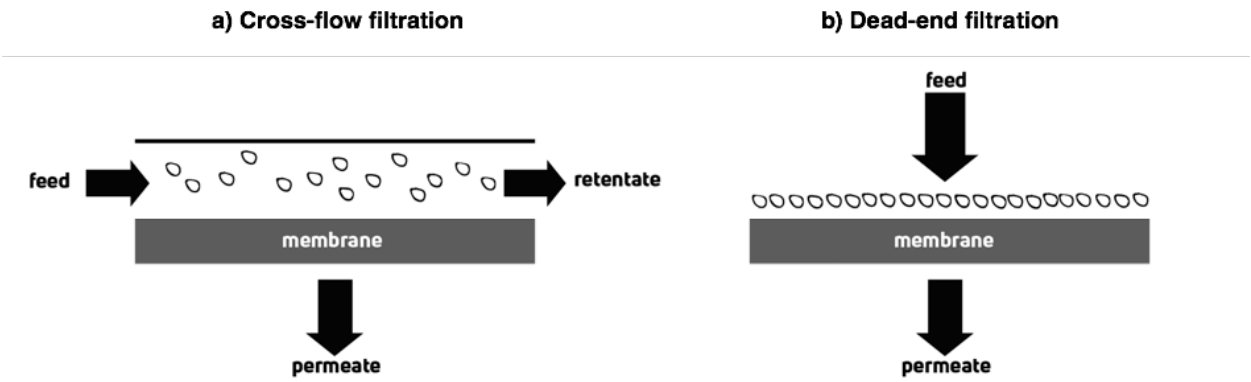


***Figure 1-2. Diagram of (a) cross-flow filtration and (b) dead-end filtration***

Cross-flow filtration is different from dead-end filtration, in which feed solution is passed through a membrane, particles are retained in the pores, and permeate is released at the other end. Cross-flow filtration got its name because most of the feed solution moves tangentially across the entire surface of the membrane, and not into the surface. The main advantage of this is that foulants (which clog the membrane) are largely washed out during the filtration process, which increases the duration of the filtration process. This can be a continuous process, as opposed to dead-end filtration [6].

## 1.3. Classification of conventional membranes

It is known that a conventional membrane is a pressure-controlled membrane that has worked well in industry [2]. The choice of membrane depends on the desired targets, the substances to be removed, and the purpose of the permeate flow [2]. Membranes are usually classified based on pore morphology,

the ability to reject certain types of composites and the materials from which they are made.

Based on their morphology, the commonly used synthetic membranes are divided into two subgroups: isotropic and anisotropic [7]. Isotropic membranes are known as symmetric membranes that have a uniform pore thickness distribution. In anisotropic membranes, also called asymmetric membranes, the properties of the pores change throughout the thickness [8]. In most of membranes processes in practice membranes consist of two layers, with different type of pore structure in each. Top layer, also called "active layer", is usually microporous ultra-thin polymeric layer, which has been placed over polymerized macroporous support layer [8]. The supporting layer is responsible for the mechanical strength of the membrane, while the top layer ensures the selectivity of the membrane (Figure 1-3).

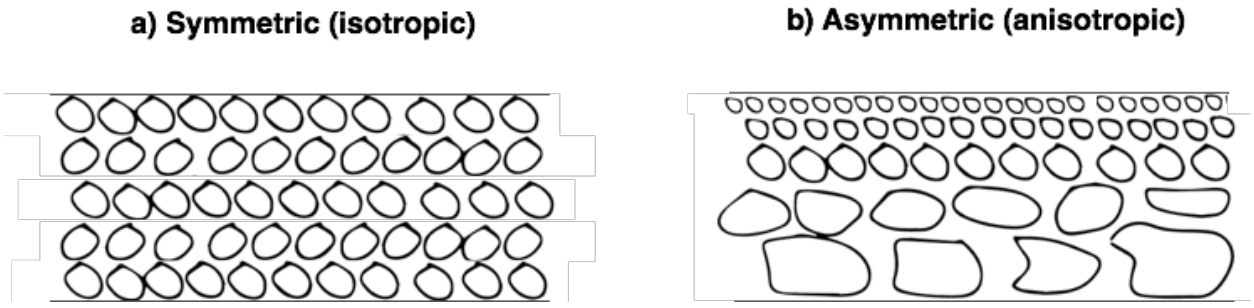


***Figure 1-3. General structure of a) symmetric and b) assymetric membranes***

This type of membrane refers to thin-film composite membranes (TFC). The main advantage of TFC membranes over other membranes is that the chemical composition and, thus, the properties of the active layer and supporting layer can be individually selected to optimize the performance of water treatment [4].

Based on the membrane pore diameter membranes are classified into three subgroups [9]:

• Macroporous membranes (d> 50 nm), applied for microfiltration and supporting layer [8];

• Mesoporous with 2<d<50 nm, used as supporting structures or in ultrafiltration water purification [9];

• Microporous with 0,5< d< 2 nm, highly selective for divalent and monovalent ions [9];

There are several types of membrane technologies in the industry, which are controlled by membrane properties and characteristics. The main conventional membrane technologies are: microfiltration (MF), ultrafiltration (UF), nanofiltration (NF) and reverse osmosis (RO)[10], as shown in figure 1-4.

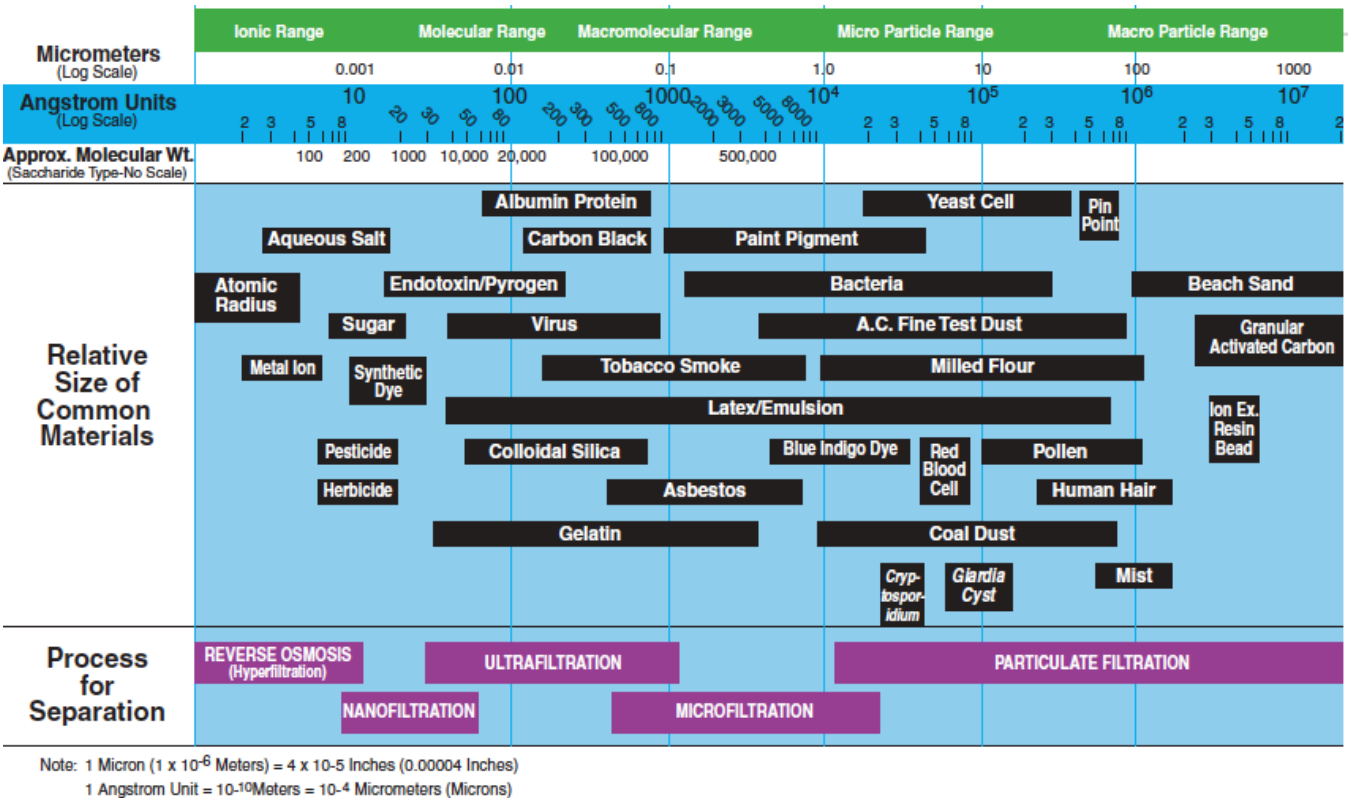


***Figure 1-4. Ranges of applications of conventional membrane technologies [10]***

Based on the size and structure of the pores, membranes can be made from different materials [6]. There is a wide range of synthetic polymers used for MF, UF, NF and RO. RO membranes are often made from cellulose acetate (CA) or polysulfone (PSf) coated with aromatic polyamides (PA) [12]. NF membranes are also made from same materials as RO, but in some cases they are made from modified UF membranes (sulfonated PSf) [12]. UF are typically made from polyvinylidene fluoride (PVDF), PSf, polyacrylonitrile (PAN), polyvinyl chloride (PVC) and polyethersulfone (PES) [12]. MF membranes are synthesized almost from same materials as UF but under different conditions [13]. In addition,

membranes can also be made of inorganic materials like ceramics or metals, for use at high temperatures or as a support [13].

### 1.3.1 Microfiltration

MF is physical filtration process based on size exclusion mechanism that uses semipermeable membrane to retain suspended particles having colloidal size with diameter from 0.05 to 1 μm [14,15]. MF is crucial part of primary water treatment, which limits the passage of pathogens and colloidal particles through pores of the membrane. In addition, this type of water treatment process is popular among consumers of membrane treatment technology showing best sales on the market [16].

### 1.3.2 Ultrafiltration

UF refers to filtration process operated at 2-10 bar pressure to separate macromolecular solutes, colloidal and microorganisms [1]. UF membranes are usually used as a pre-filtration technique for retaining process as RO and NF [5]. UF membranes are used to purify solutes varying from approximately 300 to 500000 Da, with a pore size in the range of 1-100 nm [16]. The process has been widely recognized as a substitute for coagulation, flocculation, sedimentation and sand filtration or as an autonomous system for separate regions [5, 17].

### 1.3.3 Nanofiltration

NF is diffusion controlled membrane process that is mainly applied in water treatment for “softening” purposes or , in other words it restricts flow of scale forming divalent ions ($Ca^{2+}$, $Mg^{2+}$) and some simple organic compounds [4]. Relative to UF and MF, NF is operated at high pressures: 0.5-2 MPa [16, 17]. It also has wide application for moderate nonorganic removal and high organic removal of fresh groundwater and surface water that has low dissolved content of substances in a colloidal or ionized form [17]. NF membranes have characteristics of removing substances around 1000 Da, therefore the membrane is capable of removing herbicides and pesticides [1, 10].

### 1.3.4 Reverse osmosis

RO is a high pressure water treatment process that is mainly used to desalinate seawater or brackish water [11]. RO membranes theoretically are able to remove all types of contaminants [10]. The work of RO is based on the diffusion of salts and ions against the concentration gradient [19]. Thus, to achieve this, a relatively large amount of energy is used in the reverse osmosis process at a significantly higher pressure than the above-mentioned filtration processes [20].

Based on the morphology, RO membranes are classified as asymmetric skin-type membranes and consist of polymeric materials such as cellulose acetate and aromatic polyamide [16]. In addition, the membranes have the smallest pore size

(0.3-0.5 nm), which allows to avoid the permeation of monovalent ions and organic molecules [10, 19]. Due to the extremely small pore size, RO membranes have more than 99% rejection of inorganic salts [16]. The effectiveness of RO depends largely on the performance of the membrane and the filter solution supplied.

## 1.4. Forward osmosis

Forward osmosis (FO) is the process of movement of water through a semipermeable membrane due to osmotic pressure between two solutions with different concentrations of solute [21]. In FO, a semipermeable membrane (FO membrane) is placed between the concentrated solution and the diluted solution, which are classified as feed and draw solutions, respectively (Figure 1-4) [22].

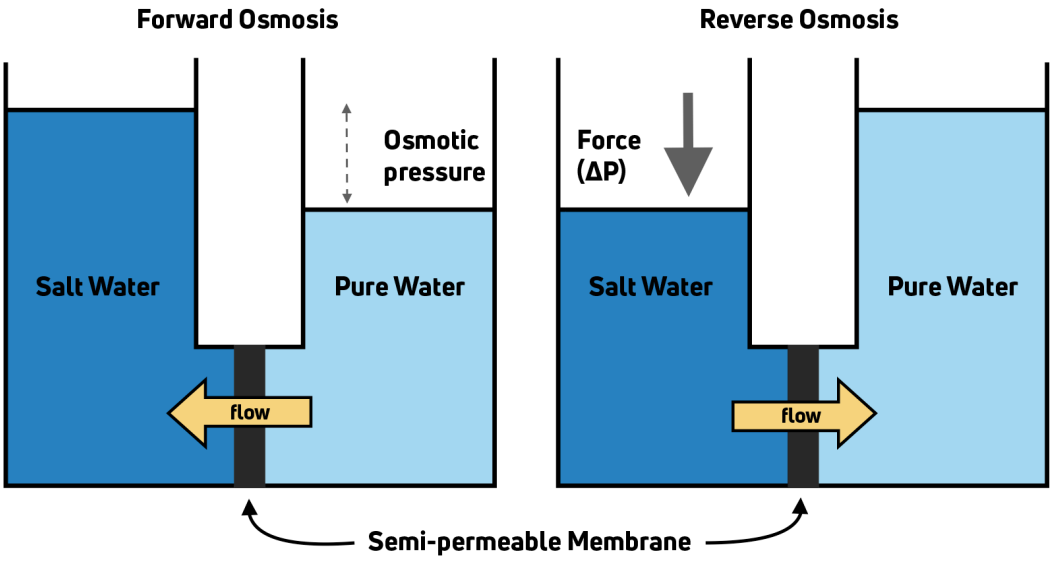


*Figure 1-5. Water flows of forward osmosis and reverse osmosis*

Using the difference in osmotic pressure to ensure water permeation through the membrane, FO can solve the main drawback of pressure-controlled hydraulic processes: the need for energy. The process of increasing availability and access to freshwater is an energy-intensive process. It is here that the natural advantage of FO arises: FO is a natural process that occurs in the cells of all living organisms and is aimed at transporting water through the cell [22]. The natural origin of direct osmosis makes it more favorable among other aforementioned traditional membrane processes, employing the difference in osmotic pressure as a driving force [22].

The theory underlying the movement of water through membrane phenomena lies in the second law of thermodynamics, which states that the degree of disorder (entropy) of an isolated system cannot decrease [21]. This means that the system is always trying to achieve maximum entropy or a state of equilibrium. In the case of two different solutions separated by a semipermeable membrane, from the thermodynamic point the water moves towards the establishment of equilibrium. Thus, in the process of direct osmosis, water is diffused so that both sides are equally concentrated.

The relationship between osmotic and hydraulic pressures and water flux is described by following simple equation:

$$J_w = A(\Delta\pi - \Delta P) \qquad (1)$$

where, $J_w$ is water flux, $\Delta\pi$ is the difference in osmotic pressures, $\Delta P$ is the hydrostatic pressure difference and $A$ is the hydraulic permeability of the membrane.

The ability of the processes caused by forward osmosis to conserve energy and supply a large amount of water has shown promising potential in water purification and desalination. However, FO membranes are subject to a number of problems, which include concentration polarization, relatively low water flow and membrane fouling [23].

### 1.5. Aquaporin incorporation

The need to modernize FO membranes has initiated several studies to optimize membrane properties, which include the use of nanoparticles as zeolites, carbon nanotubes and graphene-based materials [24]. In addition to these new chemicals, the most promising results were obtained by aquaporins. Aquaporins are transport channel proteins in the cell, which can only carry water particles and reject small molecules such as chlorides, ureas, dissolved gases and protons [24] [25]. In addition, the permeability of these protein channels can reach up to one billion water molecules per second, which is significantly superior to conventional membranes [26]. Zhao et al. [27] successfully demonstrated properties of the

modified by aquaporins with high water permeability and salt removal, which were embedded into the surface of the PA layer of TFC membrane. Thus, the obtained research results confirm the need for close attention to the development of biomimetic aquaporin membranes.

Aquaporin membranes are considered biomimetic or bio-inspired technologies. Cell membranes are barriers that allow only small particles to pass through and selectively restrict the transport of molecules such as carbohydrates and amino acids [13]. This phenomenon of transport across the cell membrane with the help of proteins is adapted for water purification and desalination processes. Currently, the manufacture of bioengineering membranes is possible by embedding aquaporin into the active layer of TFC membranes by interfacial polymerization-membrane preparation [26]. It has been shown that aquaporin-based membranes provide high permeability and selectivity, which positively impacts such aspects as performance, membrane fouling and economy.

To check whether aquaporin membranes are applicable in “realistic” circumstances, a study by Li et al. [31] modeled conditions that may affect membrane properties. Under extended conditions, membranes are usually exposed to cleaning chemicals, and therefore it is important to know how membrane properties change over time. Flow changes were caused by changes in TFC aquaporin membrane properties when hydrogen chloride (HCl), Sodium

hypochlorite (NaOCl), and sodium dodecyl sulfate (SDS) were used as chemical detergents, while Alconox (commercial anionic detergent solution) showed the greatest effect on aquaporin membrane [31]. The authors of the study concluded [31] that for all the tested cleaning agents, a very high salt removal (> 98%) was observed even after chemical cleaning. However, a significant flux change caused by chemical cleaning agents may be a potential problem of aquaporin membrane aging in future long-term deployment.

## 1.6. Fouling

Even FO has great potential in water treatment applications, there are some limitations that prevent its full-scale and continuous use. Membrane fouling appears to be the main cause of flux decline due to the accumulation of contaminants on the surface and inside the membrane [28]. In general, the membrane fouling could be divided into four main types: inorganic (mineral precipitation), colloidal (particle buildup), organic (natural organic matter and humics adsorption) and biological (biofilm formation) fouling [28, 29]. Among these categories of fouling the organic and biological fouling are considered as the most severe limitations of aquaporin TFC membranes [29].

In FO process, fouling caused by organic materials is more severe than inorganic materials [28]. Membrane organic fouling is usually initiated by cake layer formation on the membrane surface due to natural organic matter (NOM)

adsorption and deposition. In addition, more fouling problems are due to ability of NOM to easy react with other substances on the surface of membrane. Main organic foulants are known to be: alginate, humics, bovine albumin and etc.

Membrane biofouling is a dynamic process of microbial growth at the membrane surface, consequently, leading to the decline in permeability, membrane lifespan and increase of operational cost. The problem of biological fouling is caused by the formation of a biofilm containing organic macromolecules secreted by microorganisms. Such organic substances are also known as extracellular polymeric substances (EPS) that evolve on the surface as a result of settlement of byproducts of alive and dead microbial cells [30]. In an experimental study, a comparison of TFC and cellulose-based membranes in osmotic membrane bioreactors was provided by X. Wang et el. [32], it was demonstrated that several factors affect on biofilm growth, including pH, temperature and hydrophobicity. Furthermore, using confocal laser scanning microscopy combined with multiple fluorescence labeling it was found that biofoulants deposited on the FO membrane surface during long-term operation of osmotic membrane bioreactors are mainly composed of α-D-Glucopyranose polysaccharides (α-polysaccharides), β-D-Glucopyranose polysaccharides (β-polysaccharides), proteins and other organics as heteropolysaccharides, lipoproteins. As the result of biofouling in combination with organic fouling the overall loss of water flux of TFC membrane in 32 days

period dropped from around 15 to 5.5 L/$m^2$/hr (LMH). The EPS of the biofilm is altered by the complexion of divalent cations with polysaccharides, forming a bond between divalent ions and carboxyl groups of polysaccharides, thereby changing the EPS matrix into a strongly interconnected network [34]. The structure of biofilm gets denser, more stable and cohesive, while the volume and thickness of the biofilm increase. This study has shown that EPS form media matrix that enhances bacterial growth, as well as membrane biological and organic fouling which eventually influence membrane performance.

The formation of biofilm follows a phased path and includes several stages that develop sequentially. Within the first few minutes, the polysaccharides, proteins and other micro-substances form conditioning film that further facilitates attachment of free-floating protobiofilms [31]. Several hours later, the EPS contribute to irreversible biofouling and organic fouling employing dipole-dipole forces and hydrogen bonding [31]. A few hours later, constant secretion of polymeric substances leads to the formation of an organized multi-layered mature biofilm structure that is built in the EPS matrix (Figure 1-6).

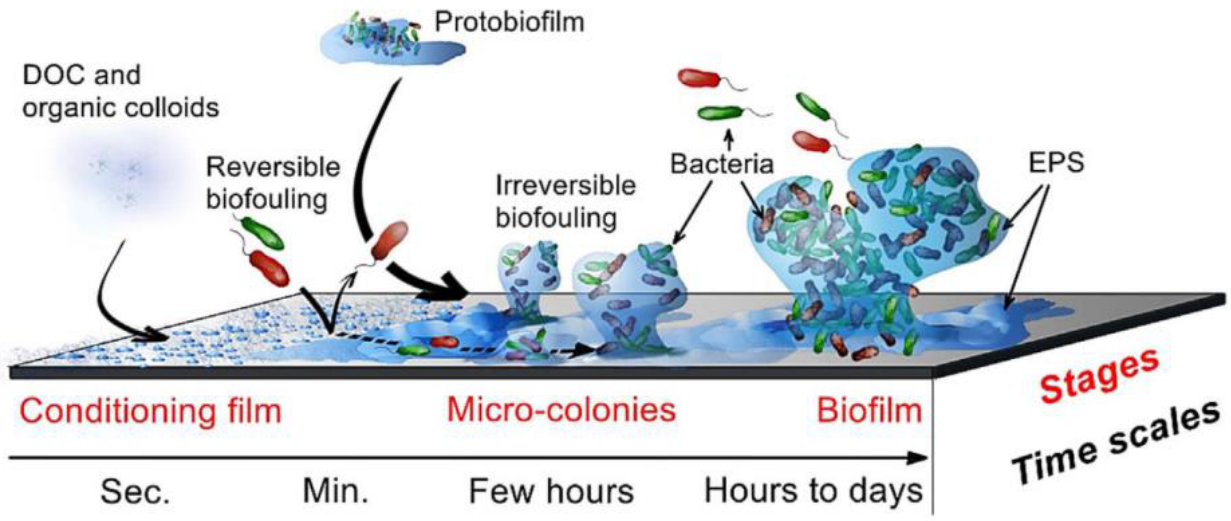


***Figure 1-6. Schematic representation of the bacterial biofilm formation on an impermeable surface [30]***

The tendency to biofouling is closely related to the characteristics of the feed solution, since it is varied by the abundance of bacteria and the presence of dissolved oxygen and organic material, as well as ionic properties and pH. High organic material and bacteria concentrations enhance the formation of conditioning cover at initial stages as a part of organic fouling [35]. The ionic strength of the feed solution can decrease the electrostatic repulsion by compressing the electrical double layer of contaminants and resulting in fouling [30] [35]. Several minutes later, such characteristics of the feed solution, as pH, as well as the availability of oxygen affect the growth rate and productivity of bacteria further [35]. It has been found that divalent cations as calcium play a key role in the biological and organic fouling, as they increase the adhesion of cells to the surface of the membrane [36].

## 1.7. Concentration polarization

As a rule, concentration polarization defines a rise in the concentration of constituents on the membrane surface that reduces effectiveness of membrane performance. This causes a decrease in the flow of water, since the local osmotic pressure change and is currently different from the osmotic pressure in the solution. [37].

One of the types of concentration polarization is internal concentration polarization (ICP), which creates crucial drawbacks in FO. ICP takes place as results of the dilution of draw solution at boundaries of the porous structure of support layer due to permeation of water through active layer. Thus, the osmotic pressure decreases at the boundary of support layer due to the dilution, and consequently, the osmotic gradient across the active layer declines as well, which causes the water flux decrease [37].

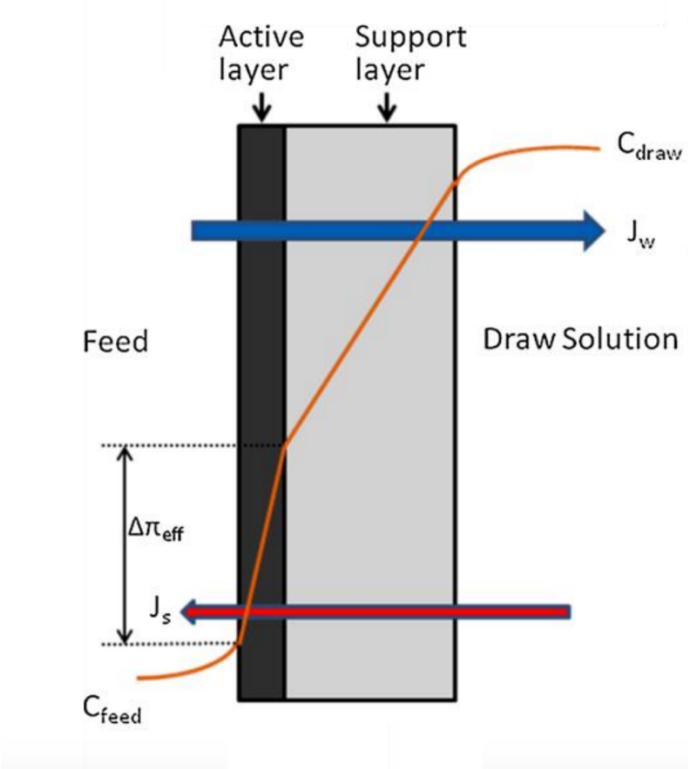


***Figure 1-7. Illustration of ICP through asymmetric FO membrane in active layer facing feed solution***

## 1.8. Fouling mitigation by silver nanoparticles

Modifications of FO membranes can be carried out by means of surface hydrophilization to reduce bacterial adhesion and organic fouling; modification of the surface for bactericidal effects and combination of both. The coatings with various chemicals are designed to hydrophilize the membrane, in order to prevent organic layer formation. To control bactericidal properties on the membrane surface anti-bacterial effect is dominated by implication of silver nanoparticles (Ag-NPs) [38].

Membrane modification using Ag-NPs is a promising option for mitigation of biological fouling of membranes. The use of silver nanoparticles has the potential to achieve the required long-term permeability of the membrane along with antimicrobial properties that limit the mutual interaction of microorganisms with the surface of the membrane [39]. Silver ions and silver nanoparticles have antibacterial properties; therefore, membranes containing silver nanoparticles can be a great advantage in wastewater treatment.

It is known that silver is toxic for a wide range of microorganisms; thus compounds based on silver were widely used in many bactericidal applications. Bactericidal mechanism of silver ions on microorganisms is well known; ionic silver strongly interacts with thiol groups of vital enzymes and inactivates them. Experimental evidence suggests that DNA loses its ability to replicate after the bacteria have been treated with silver ions [40]. Some instances of silver application should be mentioned, such as inorganic composites with a slow release rate of silver, which are currently used as preservatives in various products; another current application includes new compounds consisting of silica gel microspheres that contain a complex of silver thiosulfate that are mixed with plastics for long-term antibacterial protection. Silver compounds have been used in the medical field to treat burns and various infections [41].

Ag-NPs have antimicrobial properties due to several mechanisms. First released Ag+ could interact with disulfide or thiol groups of DNA enzymes and disrupt metabolic processes that generate reactive oxygen species or interrupt DNA replication [42]. These processes can lead to damage or death of bacterial cells. In addition, silver nanoparticles can also be attached to the surface of cells and disrupt their proper function. Finally, silver with a particle size of 10 to 50 nm are able to penetrate into the bacteria and lead to further damage by interacting with compounds containing sulfur and phosphorus [41].

## 1.9. Research significance and objectives

Although forward osmosis membranes are efficient for water purification, they suffer from formation of biofilm and cake/gel layer of organics on a surface of the membranes. Up to our knowledge, no significant research for the biological and organic fouling of aquaporin forward osmosis membranes had been performed before. Therefore, this study aims to provide important insight for biological and organic fouling of aquaporin forward osmosis membranes and impact of silver nanoparticles on their behavior. It is known that silver nanoparticles possess anti-microbial properties and can prevent potential growth of of microorganisms and EPS on the surface of the membrane. However, there is a possibility of silver particles to inhibit the functions of aquaporins, which will immediately destroy aquaporins ability to filter water molecules [43]. Therefore, for this study two

hypotheses were suggested and addressed: Whether silver nanoparticles inhibit the functionality of aquaporins; if no, whether silver nanoparticles are able to decrease organic and biofouling, which are significant drawbacks in membrane treatment processes.

To this end, this study included immobilization polyamide TFC FO membranes with covalently attached silver nanoparticles to make them less vulnerable to biofouling and organic fouling. The membranes were characterized before and after attachment for their properties and filtration performance through variety of equipment. To achieve this following tasks were carried out:

1. Synthesis of silver nanoparticles;
2. Characterization of Ag-NPs;
3. Chemical attachment of Ag-NPs;
4. Characterization of membrane, before and after modification;
5. Fouling experiments with pristine and modified membranes;
6. Cleaning of pristine and modified membranes;
7. Analysis, interpretation and explanation of results of experimental work;

# Chapter 2 – Materials and methods

## 2.1 – Materials

Calcium chloride ($CaCl_2$), sodium chloride (NaCl), alginate (ALG), Bovine serum albumin (BSA), tannic acid (TA), silver nitrate ($AgNO_3$), potassium carbonate ($K_2CO_3$), sodium citrate, potassium chloride (KCl), hydrogen chloride (HCl), potassium hydroxide (KOH) and cysteamine were purchased from Sigma Aldrich (USA). Microbiology agar used in preparing plates for disk diffusion test was obtained from Merck (USA). All chemicals in this study were used without further purification.

All glassware used (graduated cylinders, volumetric flasks, vials, media storage container, etc.) were subjected to a detergent wash followed by three rinses with distilled water. The deionized water (DI) was provided by a Milli-Q-Pad (Germany).

FO flat test “Aquaporin Inside TM” membrane sheets were obtained from Aquaporin A / S (Denmark). The membrane was manufactured by interfacial polymerization to obtain a TFC membrane and aquaporin water channels are embedded on the surface of the active layer using the Aquaporin Inside technology [44]. The active layer consists of a thin dense layer of polyamide (PA) with a

thickness of 30-100 nm, formed on the surface of a polyethersulfone (PES) layer with a thickness of 110 μm [44].

## 2.2 – Modification methods

### 2.2.1 – Synthesis of silver nanoparticles

The silver nanoparticles were synthesized based on modified protocol of Geuze and Slot [45, 46]. The synthesis process was carried out using reducing solution of TA and $K_2CO_3$, and both as reductant as well as stabilizing agent of sodium citrate [46]. A 20 ml of freshly prepared solution of sodium citrate (9.70 mM) containing tannic acid (1%, 0.1 ml) and potassium carbonate (1%, 0.1 ml) was heated to 60 °C and added with vigorous stirring to 80 mL of 69 μM $AgNO_3$ preheated to 60 °C. The mixture was placed on hot plate stirrer and boiled for 5 minutes until its color turned to dark yellow or brown. After all processes mixture cooled down at room temperature and adjusted to 100 ml.

### 2.2.2 – Attachment of Ag-NPs

Due to the advantages of using silver-based compounds to control fouling, silver nanoparticles can be successfully attached to the surface of the polyamide TFC membrane by covalent bonding using cysteamine as a bridging agent. As it is seen in Figure 2-1, the polyamide surface treated with a thiol by reacting with

cysteamine in an ethanol solution reacts with silver nanoparticles by means of chemical binding of Ag-S (TFC-AgNPs).

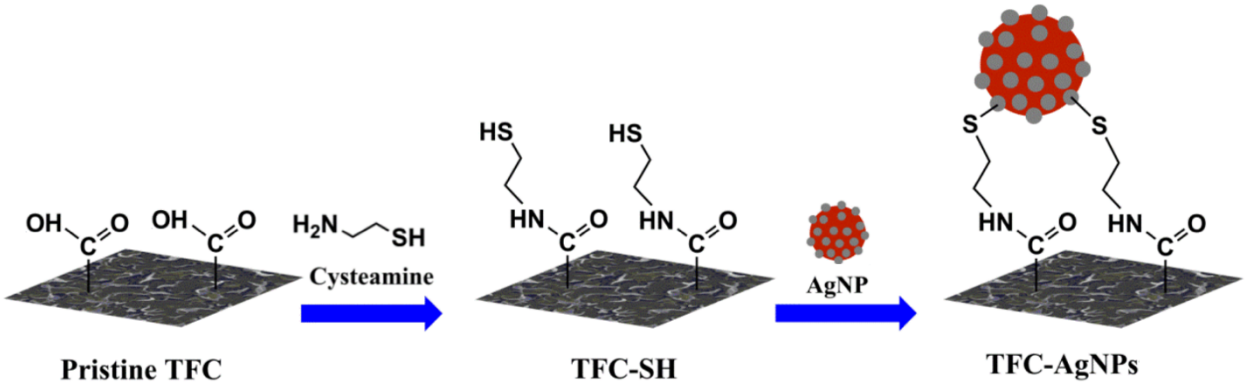


***Figure 2-1. Covalently binding of silver nanoparticles to TFC membrane [48]***

For chemical binding of silver nanoparticles TFC membrane sample was immersed in a cysteamine solution ($H_2N–(CH_2)_2–SH$, 20 mM, 50 ml) for 24 h at 50-60 °C. Then, membrane was washed with deionized water, and incubated in contact with prepared Ag-NPs suspension (50 ml) for 12 h. After all, the membrane sample was washed with deionized water and kept in distilled water at 4° C before use [47, 48].

## 2.3 – Chemical and morphological characterization

### 2.3.1 – Size and zeta potential of silver nanoparticles

Average size, size distribution and zeta potential of the synthesized silver nanoparticles were acquired with a Malvern ZetaSizer Nano ZS (Malvern

Instruments, UK) at a scattering light angle of 90 °. Size measurements were conducted in 2.5 to 4 ml polystyrene cuvettes at 25 ° C, whereas results of zeta potential of particles were obtained using folded capillary zeta cell (Malvern, UK). Size and zeta potential of particles are obtained for specific pH (from 2 to 10) range that were pre adjusted using KOH and HCl solutions.

### 2.3.2 – Zeta potential of membrane

To determine whether attachment of silver nanoparticles changes membrane properties zeta potential of the top (PA layer) surface of FO TFC membrane samples before and after modification were analyzed. Measurements of zeta potential were performed by an electrokinetic analyzer (Anton Paar, Austria) in 10 mM KCl background electrolyte solution at pH ranging from 2 to 12. The acidity and basicity of the solution were adjusted by addition HCl (50 mM) and KOH (50mM) solutions, respectively. The experiments were conducted at 25 ° C and pre-adjusted gap height between membrane surfaces of 100 μm.

### 2.3.3 – FTIR

Fourier-transform infrared (FTIR) spectra of pristine and modified membranes were acquired on a Cary 660 FTIR spectrometer from the Agilent Technology (USA). Results from spectral analysis include wave numbers varying from 500 to 4000 $cm^{-1}$ with 64 scans at a resolution of 1 $cm^{-1}$.

### 2.3.4 – Optical microscope

The surface of the TFC membrane was analyzed before and after modification under the Leica DM4000 B Microscope (Germany). The microscope utilizes different magnification (x4, x10, x40 and x100) objective lenses that are mounted on the main eyepiece lens (x10). For acquisition of surface image under 1000 magnification special immersion oil was used.

### 2.3.5 – SEM/EDX

Data collection from scanning electron microscopy (SEM) and energy-dispersive x-ray spectroscopy (EDX) of dried pristine and modified surfaces was performed by SEM Crossbeam 540 (Zeiss, Germany). SEM and EDX was used to capture membrane surfaces and to determine surface topography by scanning them with a beam of electrons. Prior the imaging of surface of the membrane, samples were covered with 10 nm gold nanoparticles. EDX analysis is an analytical method that was utilized for elemental analysis of the membranes and to identify changes between virgin and modified membrane.

### 2.3.6 – Contact angle

The measurements of contact angle between water droplet and solid surface of the membrane were collected to observe any change in hydrophilic properties after attachment of the silver nanoparticles on the TFC membrane. The experiment

was performed with aid of pipetter, that used to drop 0.05 ml of DI water on the dried surface of the membrane. Right after water drop was in contact with membrane surface the photo was taken and further used for identification of contact angle. The rise of contact angle corresponds to a decrease in hydrophilic properties and vice versa.

### 2.3.7 – XRF/XRD

X-ray fluorescence (XRF) and X-ray powder diffraction (XRD) experiment was conducted in order to investigate the presence of silver nanoparticles. The sample sizes were membranes of 2 cm in diameter. The equipment used for XRF is Max PANalytical (The Netherlands). XRD analysis was performed with aid of Rigaku SmartLab (Japan).

## 2.4 – Baseline and Fouling experiments

The baseline and fouling experiments were performed employing laboratory-scale filtration unit (CF042A-FO, Sterlitech, USA) which in combination with feed pump, draw solution pump, magnetic plate stirrer, digital scale and tanks imitate engineered forward osmosis process. The set up is designed to simulate the dynamics of larger membrane elements applied in water treatment. The schematic representation of forward osmosis set up is illustrated in figure 2-2.

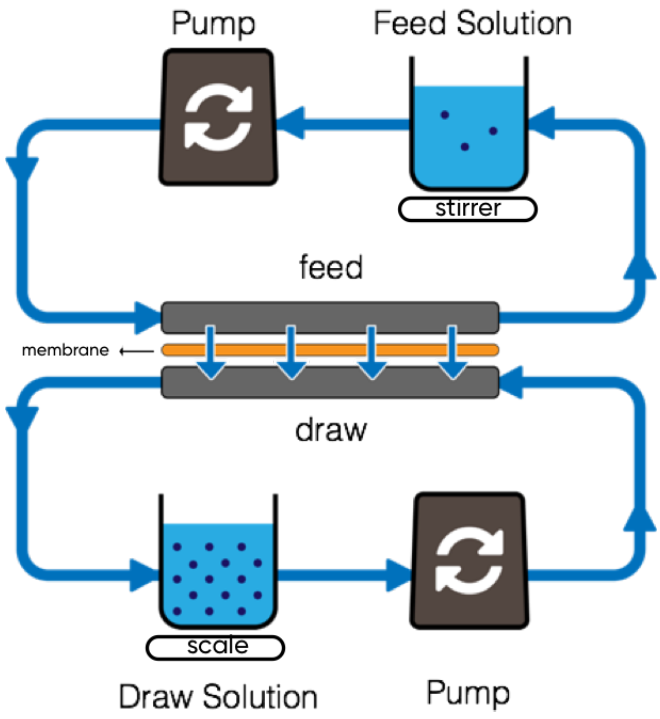


***Figure 2-2. Schematic representation of FO lab scale setup***

The draw solution is placed on the digital scale in order to take readings of change in mass, whereas feed solution is placed on magnetic plate stirrer in order to vigorously mix solution of foulants (feed). Both draw and feed solutions are connected to pumps that control cross flow velocity of streams in order to transfer solutions to inlet of membrane cell. Efficiency of aquaporin channels was tested at 12 cm/s, whereas fouling experiments were performed at 1.5 cm/s. Solutions flowing into inlet of the membrane cell are flowing in opposite directions across membrane piece which has active area dimensions of 9.2 x 4.6 cm, and the membranes were placed horizontally with active layer facing feed solution. To prevent accidental cracking or shrinkage of the membranes, the membranes were

supported from top and bottom by spacers. Each experiment began with set up set-up rinsing for 15 minutes with DI water.

In general, water flux demonstrates the productivity of membrane in unit of volume per area of membrane per unit of time (litres per meter square per hour, or LMH). Water flux is the water permeation rate across the membrane from feed solution to concentrated solution in case of FO process. As it stated above, the water flux ($J_w$) is measured by collecting mass change of draw solution over certain time interval. The following equations (2 and 3) provide how to measure water flux across the membrane and normalized flux:

$$J_w = \frac{mass\ change\ of\ draw\ solution}{water\ density * membrane\ active\ area * time\ interval} \quad (2)$$

$$Normalized\ Flux = \frac{J_t}{J_0} \quad (3)$$

2.4.1 – Effect of Ag-NPs on performance of aquaporin channels

To identify how modified membranes perform at different conditions, FO filtration experiments were conducted. Pristine membranes underwent baseline experiments in order to observe performance of aquaporin channels at different flux levels. The experiments were done at low initial flux levels and high initial flux levels to see how permeation rate can impact membrane performance. The low level flux baseline experiments were done by adjusting initial flux to 5.5 LMH,

while for high flux experiment the initial flux was set to 12.5 LMH. The concentration of NaCl has been chosen in a way to reach a certain value of initial flux.

Permeability studies were carried out in cross-flow filtration mode on pristine TFC membranes and immobilized with silver nanoparticles membranes. The measurement of water transfer through membrane from feed solution (diluted side) to the draw solution (concentrated side) with and without foulants was perfomed to observe any flux decline. Thus, it is important to perform baseline tests (i.e., filtration experiments without addition of foulants to feed solution) in order to distinct flux decline due to fouling from baseline behavior. The cross flow velocity (CFV) for all experiments was 12 cm/s and membrane orientation always was AL-FS (active layer facing the feed solution). The concentration of draw solution for each baseline experiment was preadjusted for specified initial flux. Since, the flux of membrane pieces varied from 0.5 to 3 LMH at a constant concentration of draw solution, in each case the amount of salt added was adjusted depending on the membrane sample to reach certain value of initial flux. For feed NaCl (4 L, 10 mM) solution was employed. Experiments were also performed 6 hours at an ambient temperature (23 $^{0}$C).

### 2.4.2 – Effect of Ag-NPs on cleaning of membranes

The effect of silver nanoparticles on performance of membrane after cleaning (surface rinsing, osmotic backwash and CFV magnification) processes were studied by conducting fouling experiments. In these experiments organic foulants (ALG, BSA, TA) were employed to simulate real water/wastewater. Thus, feed solution for all experiments had following concentration of compounds: 100 ppm of BSA, 100 ppm of ALG, 100 ppm of TA, 10 mM of $CaCl_2$ and 10 mM of NaCl. Whereas, draw solution was prepared by pre-adjusting concentration of NaCl solution to initial flux of 7.5 LMH.

In experiments, biomimetic membranes with and without Ag-NPs were tested in simulated membrane cleaning processes. The effect of cleaning on water flow was evaluated by conducting two consecutive runs of fouling experiments, between which a specific cleaning procedure was performed (rinsing the surface, osmotic backwashing and increasing CFV). To be able to interpret the results, the pristine membranes in the first run were fouled up to 50% flux loss, and then one of the following cleaning procedures was performed:

- Surface rinsing: increase CFV from 1.5 cm/s to 6 cm/s for 10 minutes;
- Osmotic backwash: change orientation to AL-DS for 10 minutes, at 1.5 cm/s;

- CFV magnification: increase of CFV from 1.5 cm/s to 6 cm/s for next run of fouling experiment.

It should be noted that after every 6 hour of fouling membranes underwent relaxation.

The second run of experiments was carried out under the same conditions as the first, but with a limited experiment duration of 6 hours. After completion of experiments with pristine membranes, the modified membranes were subjected to the same experimental procedures, and the results were compared with primary membranes.

### 2.5 – Antimicrobial properties of modified membrane

For antibacterial investigation suspension culture of E. coli was prepared. 1 mL of overnight E. coli culture was inoculated into a Lysogeny broth (LB) for bacterial growth in a laminar flow chamber and then placed in an incubator overnight at 37 °C with continuous shaking at 150 rpm. For the disk experiments, portion of prepared suspension culture of E. coli was spread onto several plates of bacterial growth medium. Equal portions of original and modified membranes were placed onto plates with agar in contact with active layer of the membrane. After incubation for 24 h under 37 °C the colony forming cells beneath the membrane samples were examined.

# Chapter 3 – Results and Discussion

## 3.1 – Characterization of Ag-NPs

### 3.1.1 – Size of AgNPs

The synthesized silver nanoparticles were analyzed for size distribution as a function of pH. In Figure 3-9 size of nanoparticles are plotted for pH range from 3 to 10. The graph reveals that pH conditions change does not reflect on the size of synthesized Ag-NPs. For all pH values the size of Ag-NPs is around 32 nm.

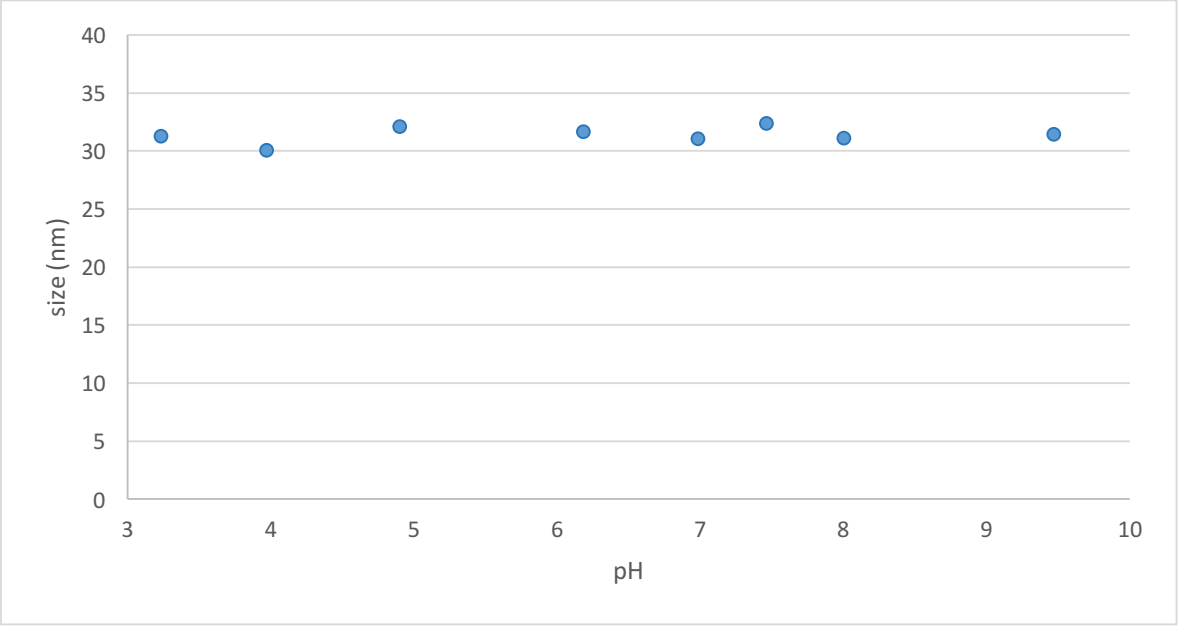


***Figure 3-1. Size of Ag-NPs as a function of pH***

pH did not affect measured nanoparticles size of synthesized Ag-NPs (Figure 3-1). The mean values of the size were ~31 nm in the pH range (3-10). This can be explained by fact that obtained nanoparticles are uncharged particles,

which do not protonate/deprotonate, depending on pH [68]. Consequently, it is expected that changes in the pH conditions will not impact the change of the diameter of nanoparticles.

### 3.1.2 – Zeta potential of AgNPs

To demonstrate repulsive properties of synthesized silver nanoparticles zeta potential measurement was carried as a function of pH (Figure 3-2).

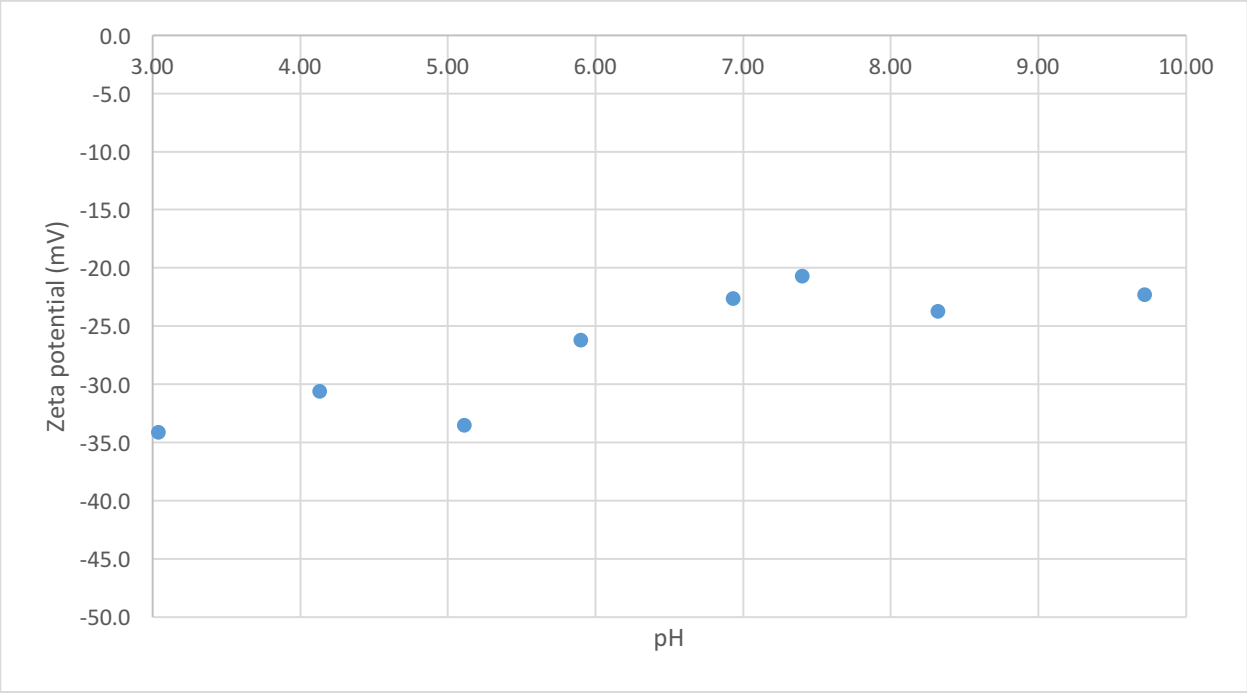


***Figure 3-2. Zeta potential of Ag-NPs as a function of pH***

The results show that as the pH decreases, the repulsive properties of Ag-NPs become slightly higher. Based on the graph, in the acidic conditions the zeta potential of the synthesized nanoparticles is -30 mV, and for the base conditions

the values of the zeta potential increase to -20 mV. In addition, it was found that the value of the zeta potential for nanoparticles at neutral pH is around -22 mV. Based on these results, it can be concluded that silver nanoparticles exhibit repulsive activity against negatively charged particles and anions and, thus, may be beneficial for the active surface of the TFC membrane.

The measurements of the zeta potential of nanoparticles show the electric potential at a shear plane of a particle [66]. As a rule, a suspension that has a potential of more positive than -20 mV is considered unstable and will lead to the precipitation of particles under certain conditions [67]. Changes of the pH of the solution from 3 to 10 did not have a significant effect on the electrical potential of the synthesized Ag-NPs (Figure 3-2). It can be stated that the synthesized NPs were stable in a wide pH range from 3 to 10. With an increase in pH, the zeta-potential of Ag-NPs became less negative from -34.1 to -20.7 mV. It is noteworthy that Ag-NPs were more stable in the pH range from 3 to 6 (the value of ZP varied from -34.1 to -26.0 mV). Synthesized AgNPs have high negative zeta potential and, therefore, they are stable over a wide pH range.

## 3.2 – Characterization of pristine and modified membranes

### 3.2.1 – FTIR

To examine whether the membrane structure has undergone changes in the chemical structure due to the attachment of silver, its composition of functional groups was analyzed using FTIR. The FTIR spectrum of the active layer can be observed in Figure 3-3.

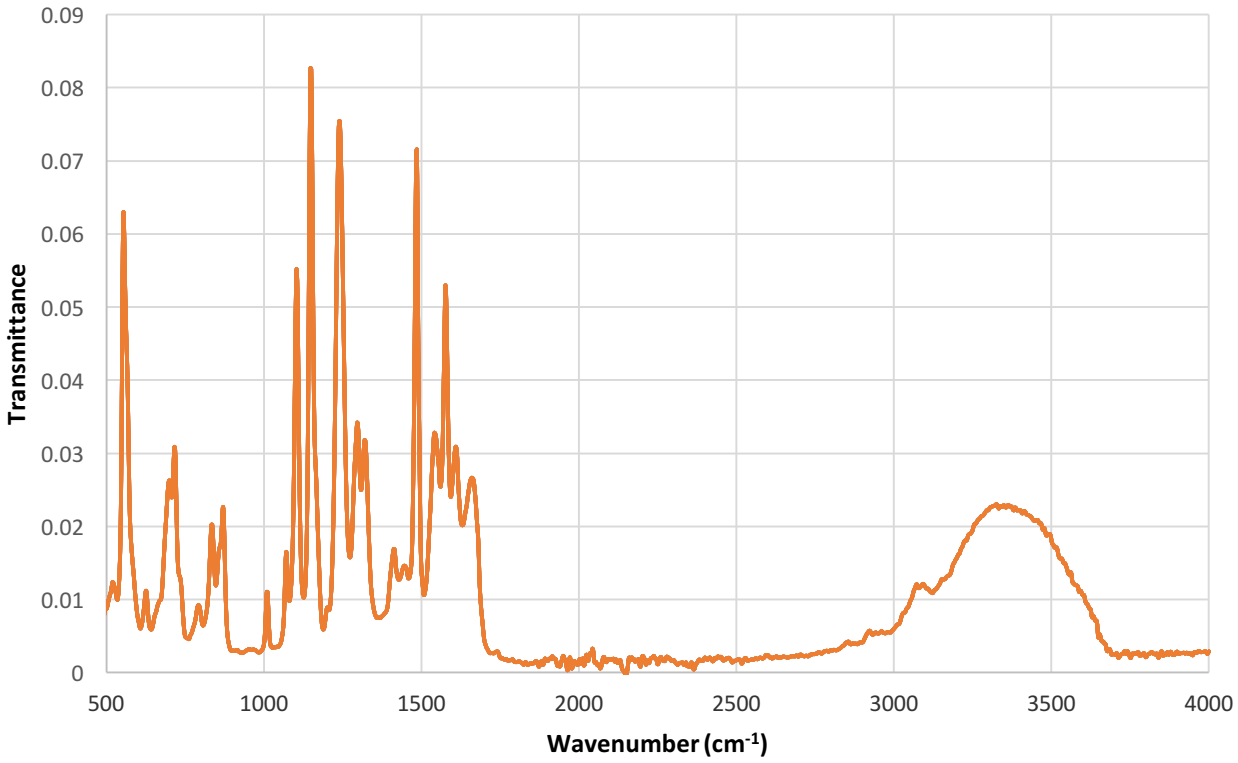


***Figure 3-3. FTIR spectrum of active layer of pristine FO membrane***

The main characteristic functional bonds of PA layer belong to the following wavenumbers: 1652 $cm^{-1}$ (C=O stretching, amide I) [49, 50]; 1608 $cm^{-1}$ (aromatic

ring breathing amide band) [51, 52]; 1577 $cm^{-1}$ (C-N stretching, amide II) [53-55]; 1413 $cm^{-1}$ (C-N stretching, amide functional group) [56], 1324 $cm^{-1}$ (C-N stretching, amide group) [57, 58]; 1074 $cm^{-1}$, 873 $cm^{-1}$, 790 $cm^{-1}$ and 717 $cm^{-1}$ (CO NH CH3, amide group [59, 60]; 3343 $cm^{-1}$ (OH stretching) [61]. The identified functional groups are presented in Table 3-1.

***Table 3-1. Functional groups of polyamide and stretchings on FTIR spectra***

| **Peak ($cm^{-1}$)** | **Functional groups** | **Reference** |
|---|---|---|
| 1652 | C=O stretching, amide I | [49, 50] |
| 1608 | Aromatic ring breathing amide band | [51, 52] |
| 1577 | C-N stretching, amide II | [53-55] |
| 1413 | C-N stretching, amide group | [56] |
| 1324 | | [57, 58] |
| 1074 | CO NH $CH_3$, amide group | [59, 60] |
| 873 | | |
| 790 | | |
| 717 | | |
| 3350 | -OH stretching | [61] |

The obtained FTIR results confirm that PA is used on the primary membrane surface (Figure 3-4), and the main functional groups were present in the analysis

spectrum, which were later used to attach Ag-NPs.

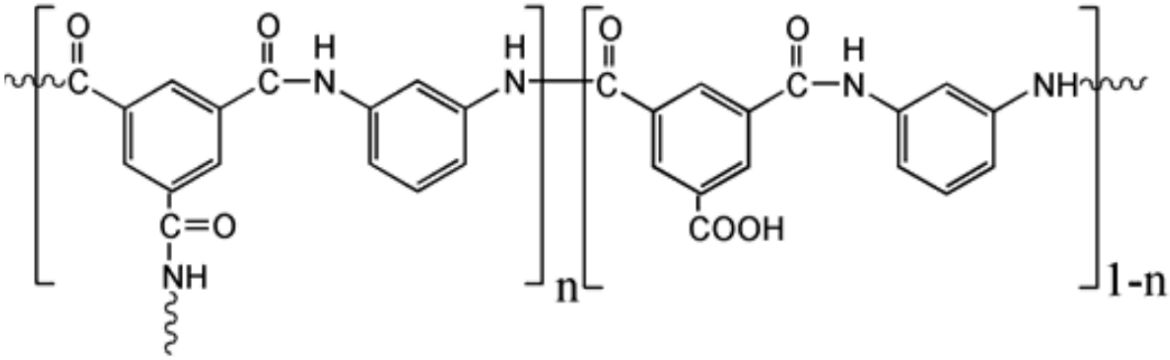


***Figure 3-4. Chemical structure of a typical polyamide used as the surface layer TFC FO membrane [62]***

The obtained spectra show no chemical changes on the active surface of the TFC aquaporin membrane after attachment of silver nanoparticles. The FTIR spectra of the active layer of membranes before and after modification can be observed on Figure 3-5. The spectra verify that top surface of the modified TFC membrane is composed of polyamide for both cases (Table 3-1).

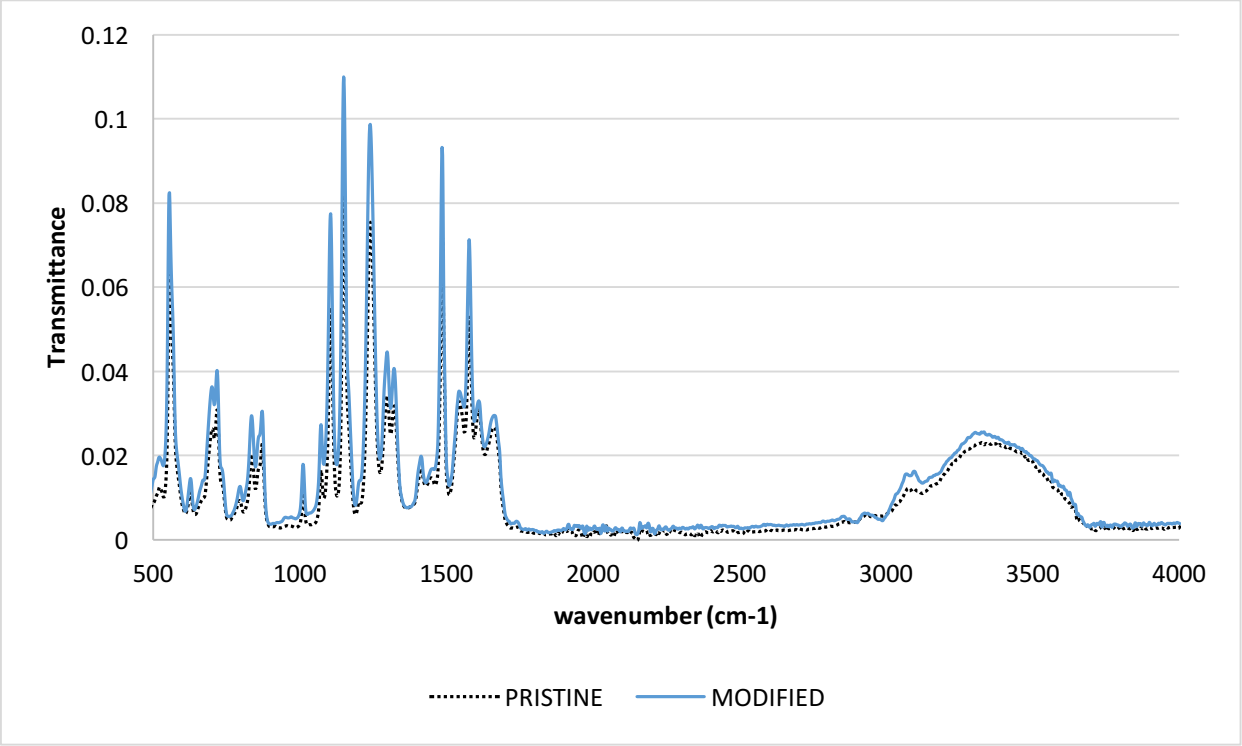


***Figure 3-5. FTIR spectra of active layer of pristine and modified TFC FO membrane***

After immobilization of the pristine membrane with silver nanoparticles, FTIR spectra on the membrane confirmed that the membrane is stable after the modification procedures and has not undergone major changes. Since the concentration of cysteamine and silver nanoparticles used for immobilization is relatively low, there are no significant changes reflected in the peaks of the FTIR spectrum. FTIR spectra (Figure 3-5) show characteristic peaks of amide I (C=O stretching), amide II (C-N stretching) and aromatic amide bond at 1652, 1577 and 1608 $cm^{-1}$, respectively, which indicates the presence of selective polyamide layer. In general, the FTIR results show that, after modifying the

membrane, it retained the pre-existing functional groups that the original membrane had.

### 3.2.2 – Zeta potential

The main purpose of the analysis of zeta potential is to obtain information about the surface charge of the membrane, which is established upon contact with water. The pH dependence provides information on the presence of acidic or basic functional groups on the membrane surface, which is important for analyzing the ability of a membrane to deflect negatively charged ions and attract positive ions, which are the result of dissolved salts [63]. Thus, from Figure 3-6 it can be seen that as pH gets higher the zeta potential of membrane increases.

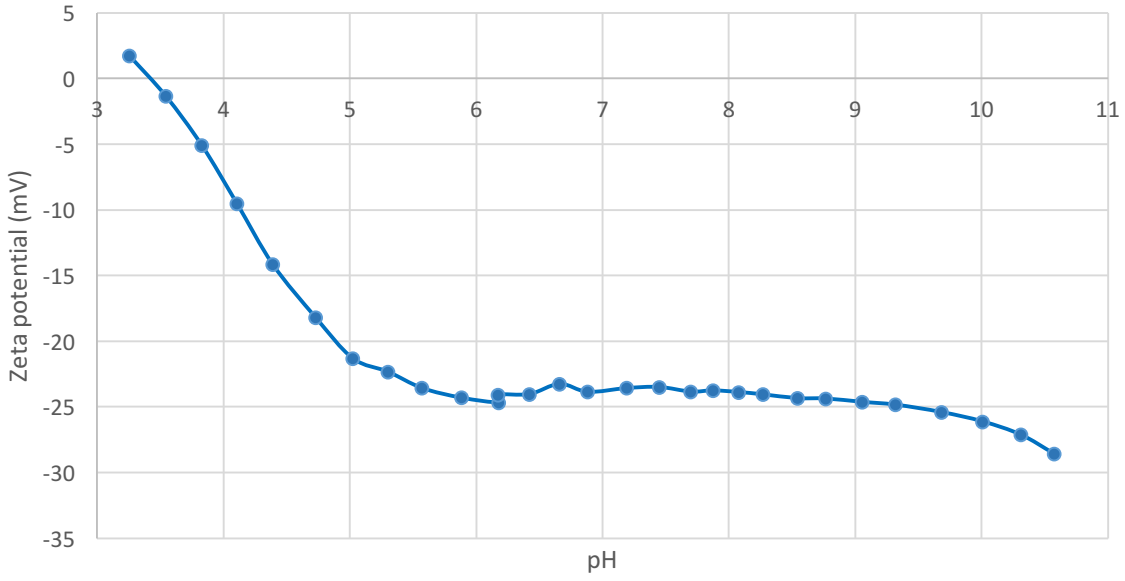


***Figure 3-6. Zeta potential of pristine membrane for 1mM KCl electrolyte solution as a function of pH***

The graph (Figure 3-6) demonstrates zeta potential measurements of the membrane surface of pristine membrane for pH range from 3 to 11 in the presence of 1 mM KCl as a background electrolyte solution. The solution pH was adjusted using HCl (50mM) and KOH (50 mM) solutions.

It can be observed that the reading of the zeta potential for pH 3.26 is 1.73 mV, then it drops to -24.66 mV at pH 6.18 and remains almost constant for a pH in the range up to 10.533. In addition, at a neutral pH, the zeta potential reading is -23.42 mV. The demonstrated negative zeta potential values verify that the dissolved ions will be affected by a remarkable electrostatic repulsion force, which consequently provides salt rejection by membrane surface.

The graphs (Figure 3-7) demonstrate zeta potential measurements of the membrane surface after modification membrane for pH range from 3 to 11 in the presence of 1 mM KCl as a background electrolyte solution.

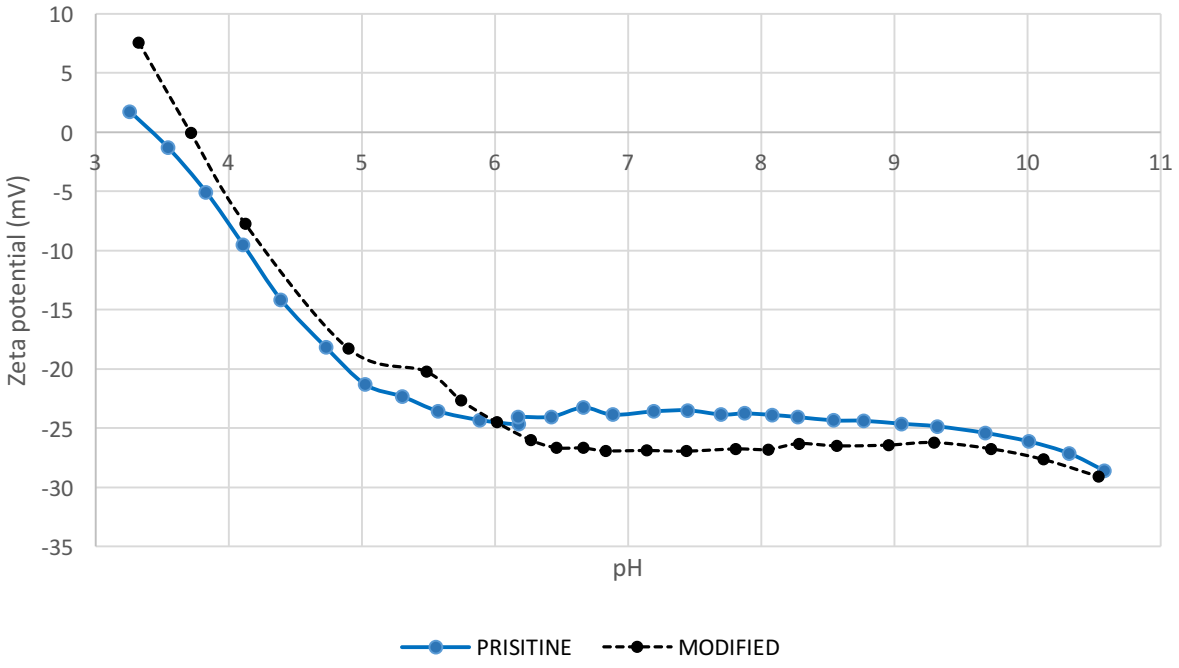


***Figure 3-7. Zeta potential of pristine and modified membranes for 1mM KCl electrolyte solution***

It can be observed that there is no significant difference in charge of the surface after modification membrane with silver nanoparticles. For modified membrane, zeta potential is 7.59 mV at pH 3.23 decreasing till -26.62 (pH 6.46) and remains constant as in the case of the pristine membrane. In addition, at neutral pH the zeta potential readings are -23.42 mV and -26.54 mV for pristine and modified membranes, respectively.

The values obtained from measuring the zeta potential confirm the repulsive properties of pristine and modified membranes. These results indicate that repulsive electrostatic double layer interactions will develop between the membrane and the negatively charged surfaces of the pollutants during fouling

experiments. Thus, both pristine and modified membrane must have repulsive properties.

In general, the charge on the membrane surface is formed due to dissociation or protonation of functional groups of the membrane [69]. The obtained zeta potential for pristine and modified membranes verifies protonation process of polyamide functional groups at low pH range. At acidic conditions, amine groups remained from interfacial polymerization (verified by FTIR, N-H stretching 3353 $cm^{-1}$) were protonated while the carboxylic groups did not undergo any changes [69, 70]. When acidity of the solution has increased, the carboxylic group dissociate in contact with solution and membrane surface becomes negatively charged.

Above results indicate that the zeta potential of the TFC membrane did not change considerably after silver attachment, which might be explained by same surface charge of silver nanoparticles (Figure 3-7) and low concentration of silver nanoparticles employed. However, small enhance of surface charge repulsion of a modified membrane can be ascribed to silver nanoparticles attachment exhibiting negative charge due to the surface oxidization [72]. Thus, Ag-NPs may contribute to surface repulsion of anions and negatively charged particles, resulting in better rejection of salt and foulants.

### 3.2.3 – Optical microscopy

Figure 3-8 demonstrates surface photographs of pristine PA layer of the TFC membrane before attaching silver nanoparticles.

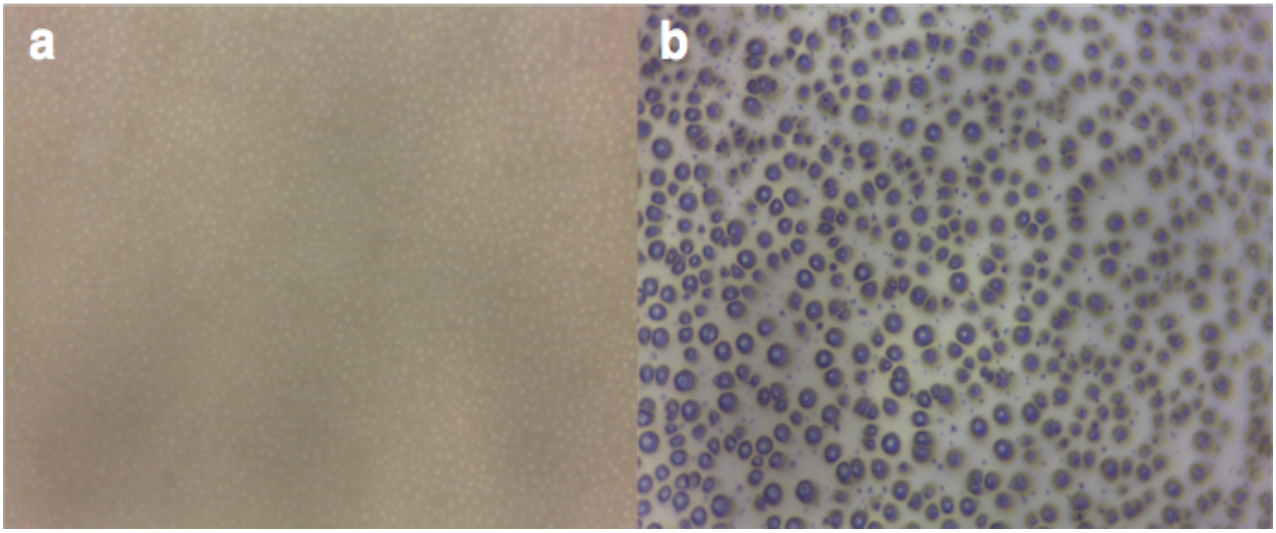


***Figure 3-8. Optical microscope images of active layer of pristine FO membrane under a) x400 magnification and b) x1000 magnification***

Both photographs show that the membrane has porous channels on the membrane surface, which can be called aquaporin channels. The first image (Figure 3-8a) was taken at a magnification of 400 times, showing well-dispersed pores in the focusing zone of the membrane. With a more thorough study (x1000) (Fig. 3-8b) one can observe the pores of the membranes. The pores are of various sizes and are well distributed throughout the membrane. It should also be noted that prior to modification, the pristine membrane is grayish in color and does not contain any impurities or other substances.

The pictures of silver attached TFC membranes are shown in figure 3-9.

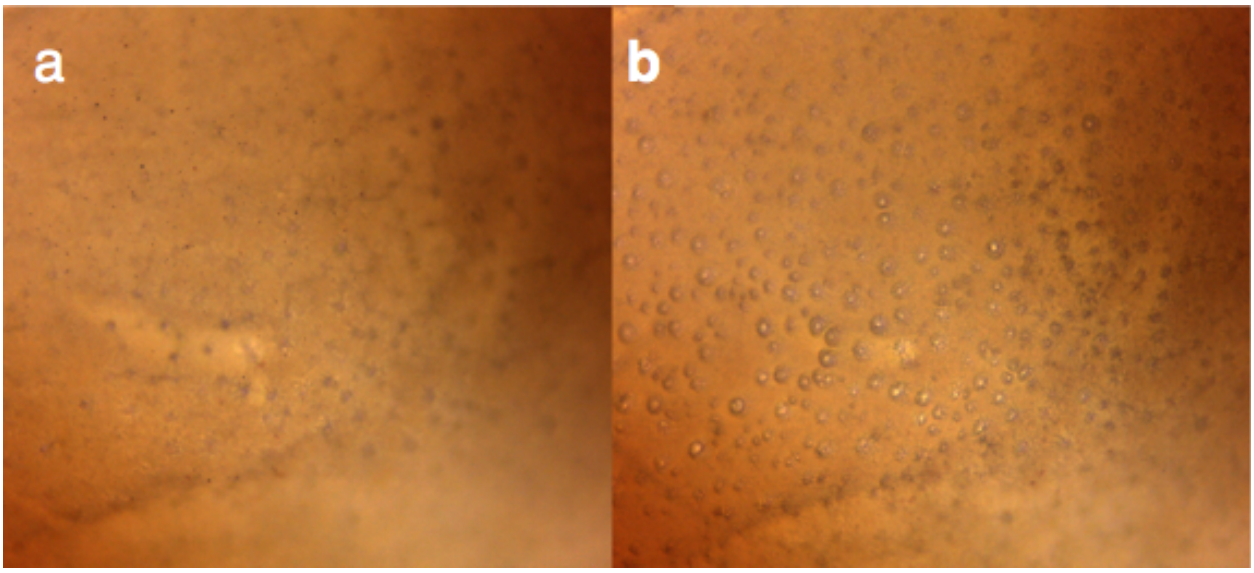


***Figure 3-9. Optical microscope images of active layer of modified FO membrane under x1000 magnification a) focusing on a surface and b) focusing on pores***

After reaction with silver nanoparticles, the original white TFC membrane turned yellowish, indicating silver is successfully attached to the surface of the membrane. The results from the optical microscope make it possible to take photographs with different focal lengths. Figure 3-9a shows the presence of tiny little dark points on the surface, which are most likely silver nanoparticles. Another photograph (Figure 3-9b) shows that the pores remain the same as in the original conditions, while maintaining the structural integrity of the membrane.

### 3.2.4 – Contact angle

The measurement of the contact angle is carried out to assess the effect of the attachment of silver nanoparticles on the hydrophilicity of the membrane. As

the contact angle of the surface decreases, the membrane's hydrophilicity improves. According to the data obtained, the average angle of contact with water of the active layer of the pristine membrane is 49 °, which demonstrates fairly hydrophilic properties. This is the base result for comparison purposes to characterize the modified membrane.

According to the acquired contact angle data after silver attachment, Figure 3-10 shows the contact angle of the membrane decreasing from 49° for the pristine polyamide layer to 45° for the incorporated with silver membrane surface, demonstrating that the modification by AgNPs provides almost same hydrophilic properties.

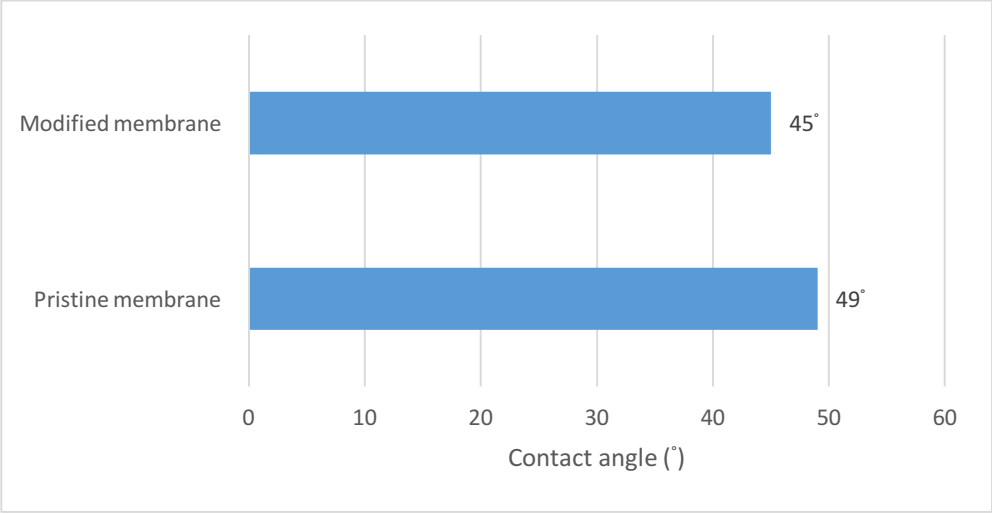


***Figure 3-10. Contact angle measurement of active layer for pristine and modified membranes***

The values of the contact angle of the active layer before and after the modification do not detect the effect of silver immobilization. The contact angle of a pristine and modified membrane gives almost identical results. The effect of adding Ag-NPs is weakly correlated with hydrophilic properties. This may be due to the fact that there was not enough silver to observe any changes in the properties of the membrane. It can be concluded that Ag-NP does not affect the hydrophilicity of the membrane.

### 3.2.5 – SEM/EDX

High resolution SEM image of an active layer of TFC FO membrane was obtained for a pristine membrane that reveals a “ridge and valley” structure of the surface (Figure 3-11).

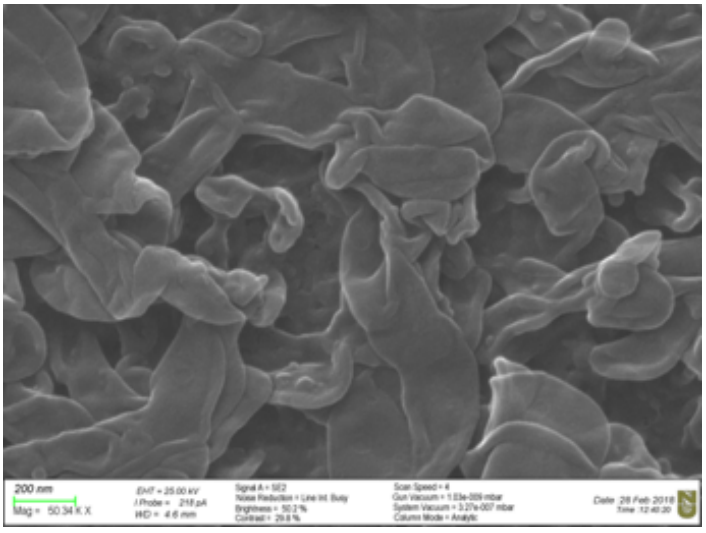


***Figure 3-11. SEM image of PA layer of pristine TFC FO membrane under x50k magnification***

Furthermore, the elemental composition of pristine membrane was obtained using EDX analysis. EDX spectrum (Figure 3-12) of pristine surface before modification procedures demonstrates the presence of such elements as carbon (C, 8.0%), sulfur (S, 0.5%), oxygen (O, 1.5%) and shows absence of silver (Ag).

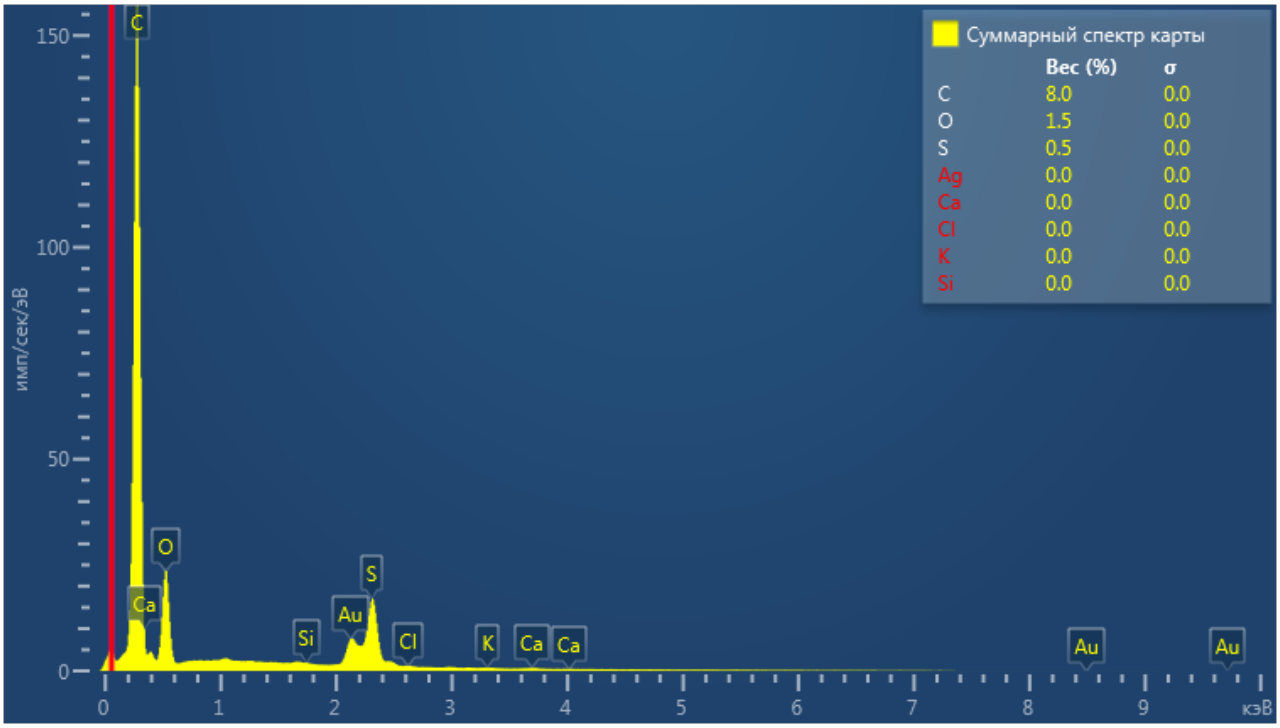


***Figure 3-3. EDX spectrum of pristine TFC FO membrane***

The results of the SEM confirm the change in the morphology of the surface attached to the nanosilver as compared to pristine membranes (Fig. 3-13). Figure 3-13 shows the scattered spherical particles on a valley-like structure with a diameter of about 30 nm, which is consistent with the measured size of the

nanoparticles, which suggests that silver nanoparticles were present on the modified surface of the TFC membrane.

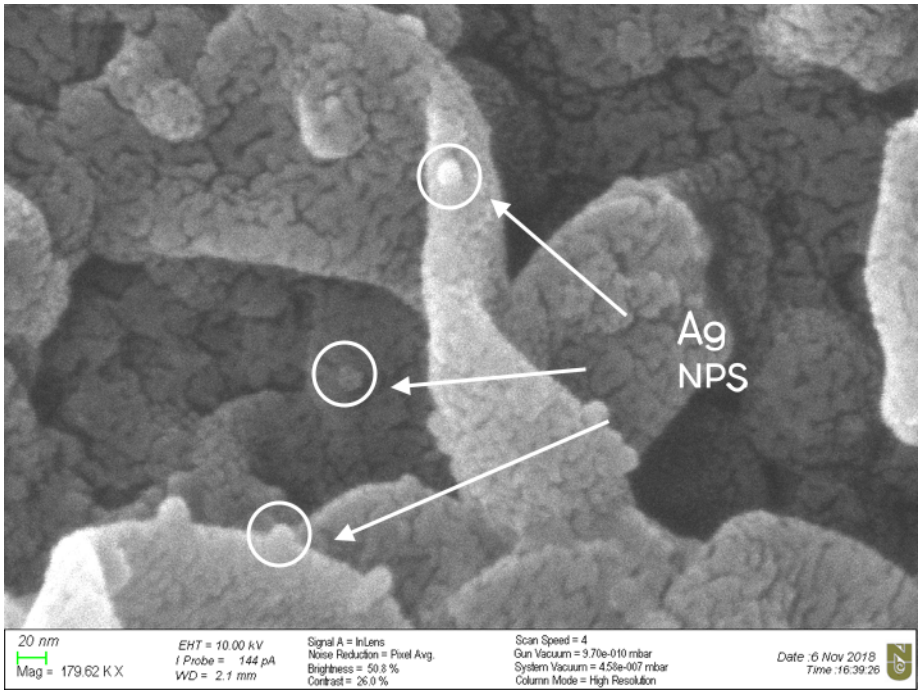


***Figure 3-13. SEM image of polyamide layer of modified TFC FO membrane***

Furthermore, EDX spectrum of modified surface demonstrates the presence of silver, confirming the attachment of AgNPs on the membrane surface. The weight percentage of silver presented spots is 0.1%, confirming low concentration of silver in the structure of membrane. Besides silver nanoparticles, EDX spectra have shown presence of carbon (C, 7.8%), oxygen (O, 1.5%) and sulphur (S, 0.5%) (Figure 3-14).

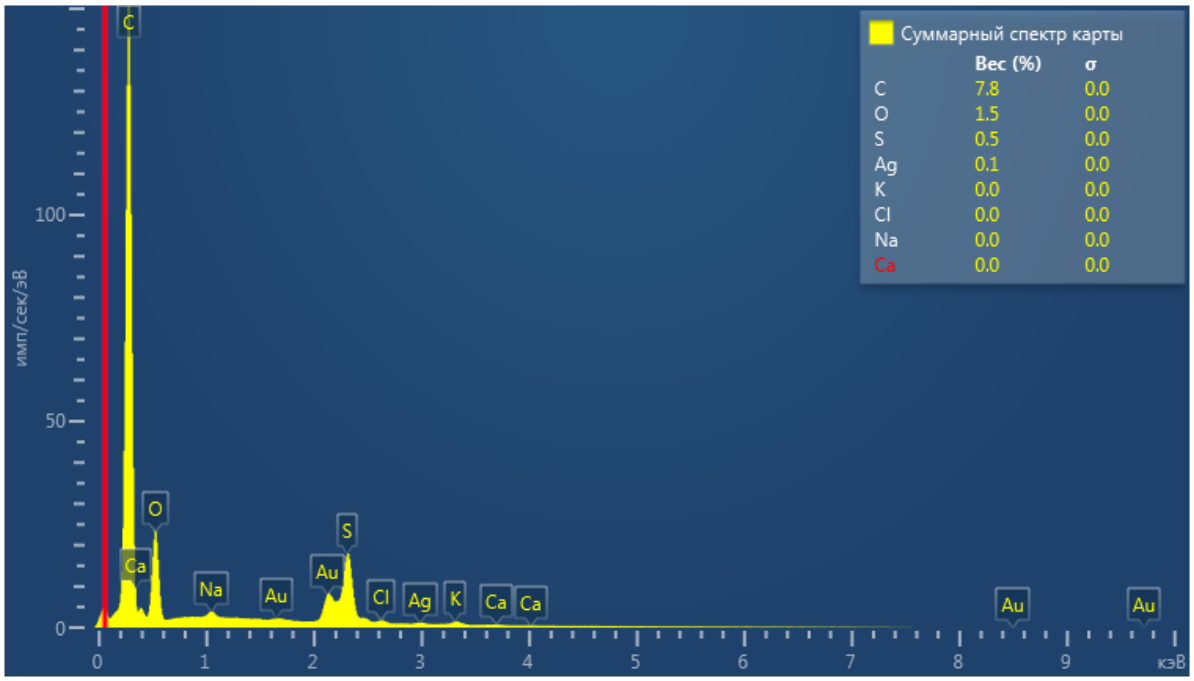


***Figure 3-14. EDX spectra of modified TFC FO membrane***

Both microscopic analysis methods (optical microscope and SEM) show successful modification of the TFC FO membrane. The first indicator of successful attachment of silver on the membrane was a change in the color of the membrane surface from gray to dark yellow. In addition, a uniform color indicates a uniform distribution of Ag-NPs on the membrane. A comparison of photographs from an optical microscope shows that the pores on the surface have retained their physical integrity. A further successful modification is shown by SEM analysis, which at high magnifications showed the presence of silver deposits on the surface of the polyamide layer. The EDX spectra of intact and modified membranes confirmed the presence of silver after the modification processes.

### 3.2.6 – XRF and XRD

Figure 3-15 presents the composition of some elements in a pristine membrane before attachment of silver nanoparticles. The elemental composition of a pure membrane consists mainly of sulfur (S, 86.508 %), oxygen (O, 4.570%), chlorine (Cl, 3.365%), calcium (Ca, 1.943%) and other elements.

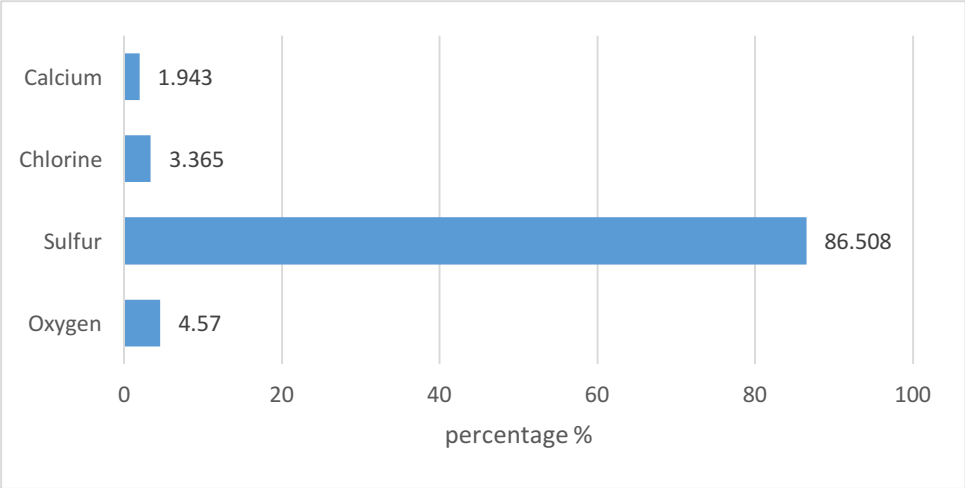


***Figure 3-15. XRF results of active layer of pristine TFC FO membrane***

According to the results from XRD (Figure 3-16), there are three reflections at 2θ = 18º, 23º and 26º, corresponding to peaks associated with the crystal planes (200) and (002) of the α-phase of the polyamide [64]. According to the literature, these crystal planes have also been discovered and verified as polyamide [64, 65].

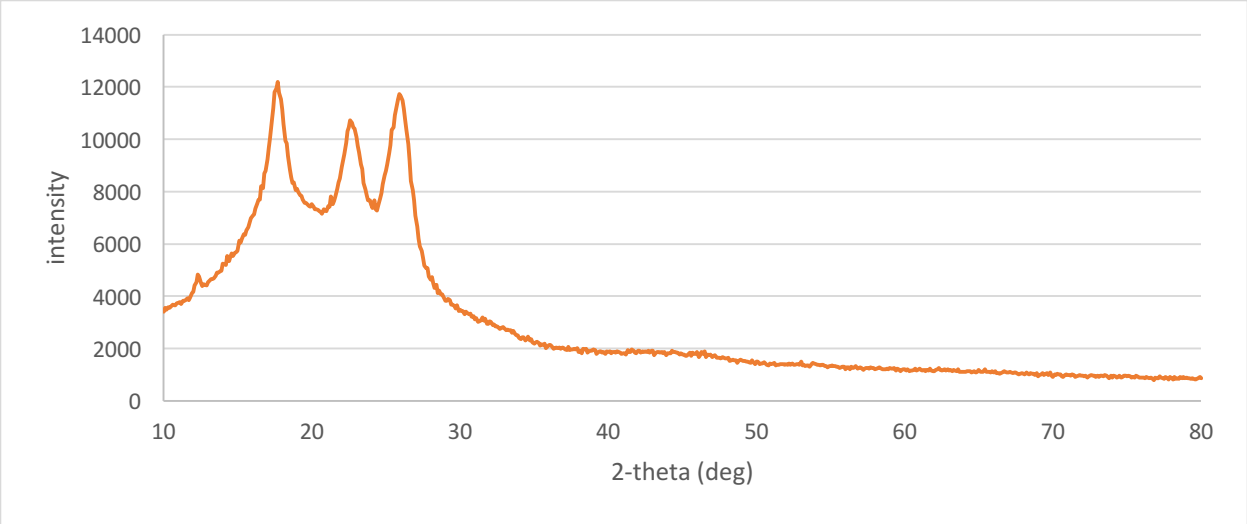


***Figure 3-16. XRD results of active layer of pristine TFC FO membrane***

The results obtained after modification from XRF analysis (Figure 3-17) shows the composition of some elements in a modified membrane after attachment of silver nanoparticles.

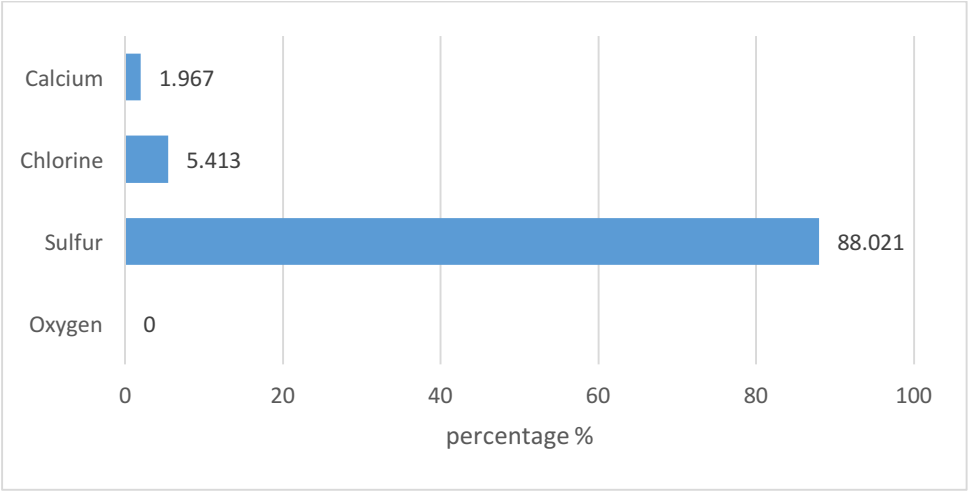


***Figure 3-17. XRF results of active layer of modified TFC FO membrane***

The elemental composition changed as a result of the reaction of the membrane with cysteamine and the further attachment of silver nanoparticles. It can be seen that the percentage of sulfur and chlorine in the membrane structure increased by about 3%, which may be due to the thiol group being attached to the TFC membrane for reaction with nanoparticles.

However, the composition obtained from the results of XRF, in contrast to previous results, does not detect the presence of nano silver. This can be explained by the limitations of XRF analysis, which cannot detect traces of particles with extremely low concentrations. However, an increase in the sulfur content shows that, after reaction with the cysteamine membrane, thiol groups appeared in its structure, which were later used to attach silver.

The XRD pattern after immobilization for silver nanoparticles show broad peaks at around 18°, 23° and 26°. This is almost same pattern as in the case of pristine membrane, except for the small shift at 38°. The XRD spectrum of pristine and modified membranes are shown below (Figure 3-18).

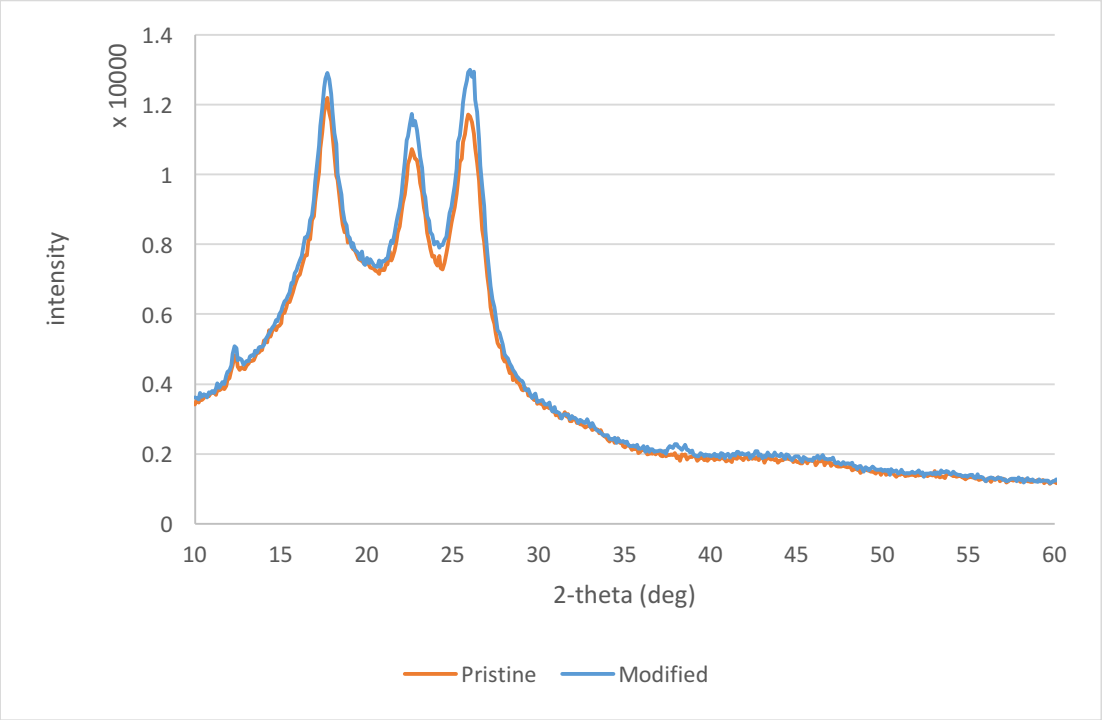


***Figure 3-4 XRD results of active layer of modified TFC FO membrane***

## 3.3 – Antimicrobial properties of membrane

The results of incubating 1 cm piece of pristine and modified membranes for 24 hours in nutrient agar with E. coli bacteria are illustrated in Figure 3-19, where pristine polyamide layer of the original membrane had no effect on inhibition of E. coli growth on the membrane surface.

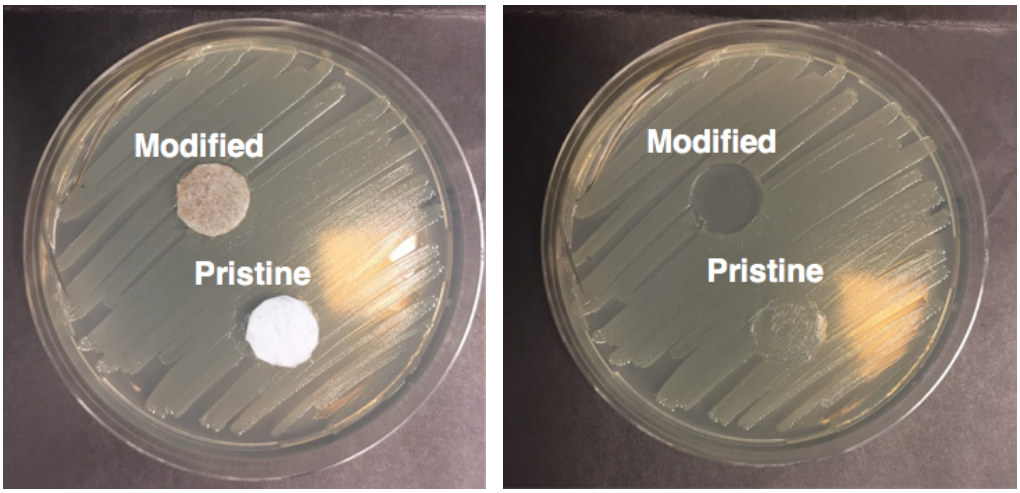


***Figure 3-19. (a) Disk experiments before removing membrane samples. (b) Disk experiments after removing membrane samples. Incubation duration – 24 hours. E.coli bacteria in LB agar broth.***

The photograph under pristine membrane sample shows growth of bacteria. Whereas the Ag-NPs immobilized membrane disk demonstrates antimicrobial properties by showing clear LB surface under the membrane sample. Furthermore, the easy growth of bacteria on the surface of pristine membrane suggests vulnerability to biofouling of polyamide surface and need for antibacterial protection. Based on the appearance of inhibition zone under modified membrane, it can be stated that attachment of silver nanoparticles on surface creates biocidal properties of the membrane.

It can be observed that the modified membrane exhibits clear growth inhibition zones, representing considerable antimicrobial activity against bacteria. In the case of a pristine membrane, no growth inhibition zones were observed

under membrane, which implies that the original membrane has no activity against bacteria. The results show that embedded silver nanoparticles impart effective antimicrobial activity to the TFC FO polyamide membrane. Appearance of such property can be explained by two mechanisms. The first mechanism is based on the ability of Ag-NPs to disrupt the correct function of the plasma membrane potential and reduce the levels of intracellular ATP (adenosine triphosphate), which leads to the destruction of the cell membrane [74]. The second mechanism of the antimicrobial properties of silver is due to the release of Ag + ions by nanoparticles, which lead to the interaction of thiol or disulfide groups of DNA or enzymes [75, 76]. Subsequently, this leads to a stop in the functioning of the metabolic processes of bacteria. Thus, FO membrane has successfully gained antimicrobial property.

### 3.4 – Effect of Ag-NPs on performance of aquaporin channels

Figure 3-20 demonstrates the graph of water flux change for baseline experiments for pristine and modified membranes.

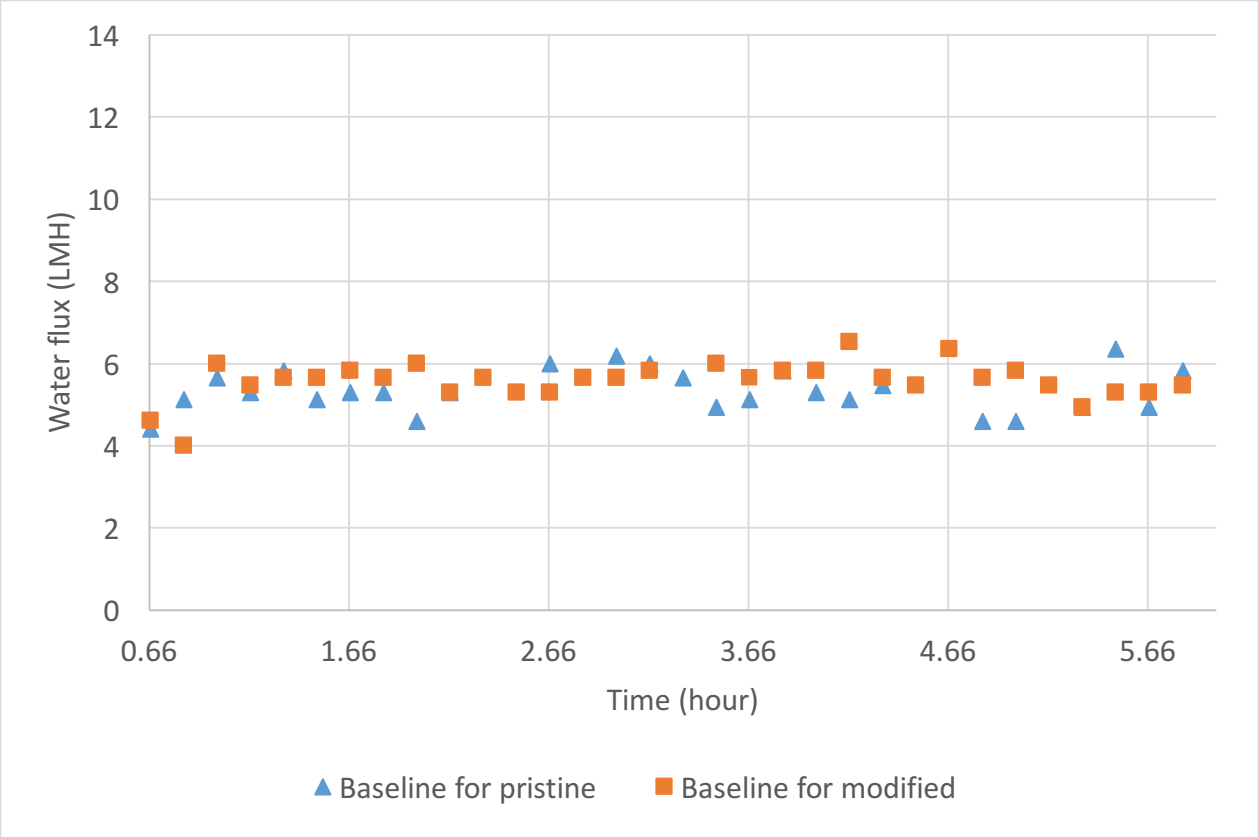


***Figure 3-20. Low flux levels FO baseline experiments for pristine and modified membranes. AL-FS orientation at 12 m/s CFV in a cross flow mode. Feed 10 mM NaCl, draw pre-adjusted NaCl solution.***

From the obtained results it can be seen that the baseline tests for both types of membranes show an almost constant change of the water flux. Both plots for baseline and modified baseline tests vary between 4.6 and 6.3 LMH, showing an average of 5.5 LMH. Both types of the membranes of modified and pristine membranes were subjected to the same experimental conditions, resulting in almost the same water flux. Since the purpose of the experiments was to observe the ability of aquaporins to permeate water, when the draw solution was adjusted

to ensure a relatively low water flux, it can be stated that the modified membrane has the same properties as the primary membrane.

The effect of higher flux on performance of modified membrane is shown in Figure 3-21.

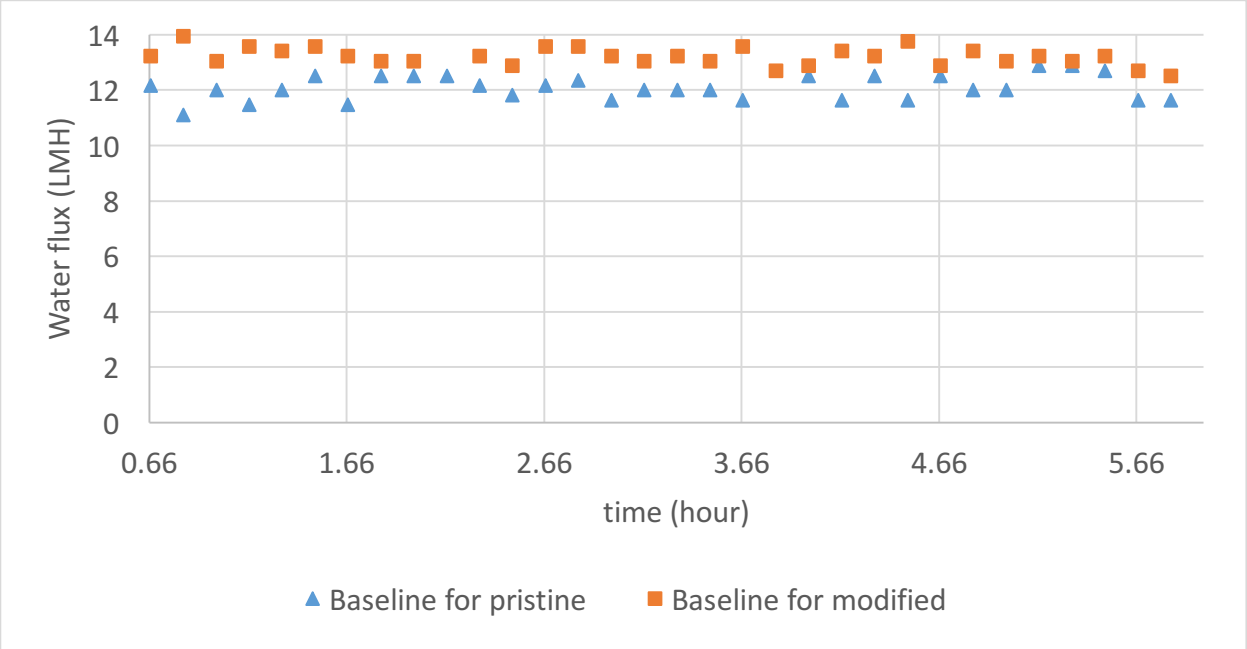


***Figure 3-21. High flux levels FO baseline experiments for pristine and modified membranes. AL-FS orientation at 12 cm/s CFV in a cross flow mode. Feed 10 mM NaCl, draw pre-adjusted NaCl solution.***

Experiments were performed starting from an initial flux of around 13 LMH. As in the case of lower flux, the baseline tests at 13 LMH show almost constant results. For baseline tests it is observed that flux varies from 11 to 14 LMH for 6-hour filtration period, showing approximately 12 LMH average flux for the pristine membrane and 13 LMH average flux for the modified membrane. The results

confirm that the membrane with Ag-NPs did not lose ability to filter water at high water flux.

The purpose of baseline experiments for the membrane before and after the attachment of silver nanoparticles was to determine whether Ag-NPs disrupt the functionality of aquaporins water channels or not. Based on the results obtained, it can be stated that silver nanoparticles do not eliminate the ability of membranes to permeate water through. In both experiments with pre-adjusted draw solutions (5.5 LMH and 12.5 LMH), the behavior of the FO membranes was not affected. It should be added that the characteristics of the modified membrane under baseline conditions (i.e, different concentrations of NaCl solutions as draw and feed solutions) do not correlate with the use of AgNP, therefore in this case silver nanoparticles cannot be considered as aquaporin membrane inhibitors. It also does not exclude the fact that the number of particles was so small that it did not affect the large-scale properties of the membrane.

### 3.5 – Effect of Ag-NPs on cleaning of membranes

Before performing the fouling experiments membrane underwent baseline experiment (Figure 3-22).

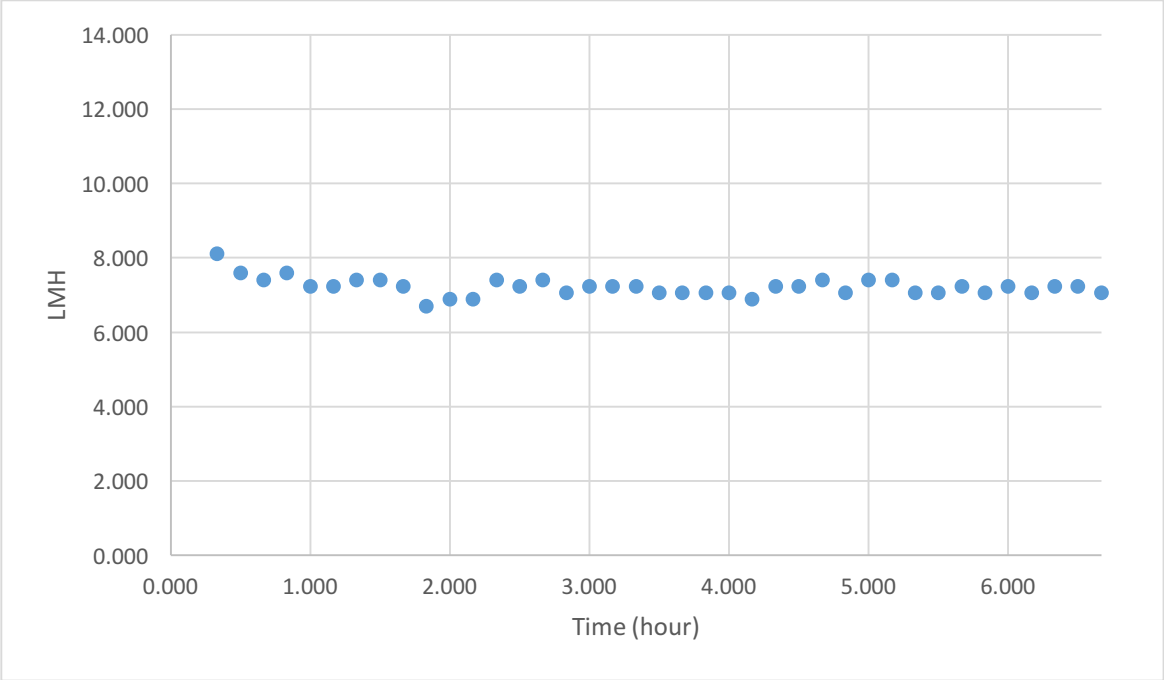


***Figure 522. FO baseline experiments for pristine membrane. AL-FS orientation at 1.5 m/s CFV in a cross flow mode. Feed 10 mM NaCl, draw pre-adjusted NaCl solution.***

### 3.5.1 – Surface rinsing

Figure 3-23 shows the normalized flux of the pristine membrane, which was subjected to a 50% flux loss during the 18-hour fouling experiment, followed by a surface wash cleaning procedure to observe how the membrane is able to recover during the next 6-hour fouling experiment.

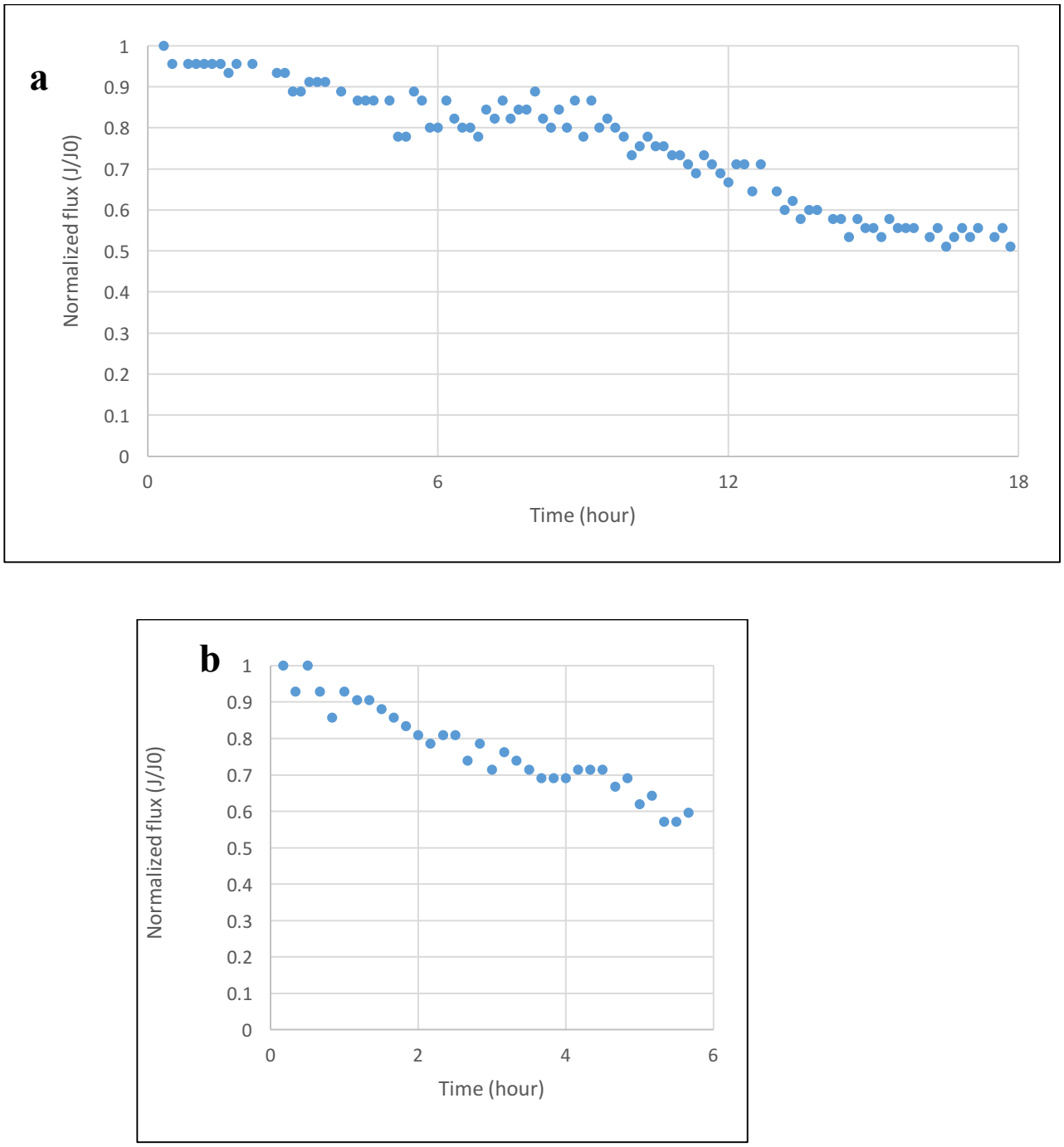


***Figure 3-23. Normalized water flux of fouling experiment for pristine membrane: a) before surface rinsing and b) after surface rinsing. Experimental conditions for fouling experiments: feed solution (mixture of ALG (100 ppm), BSA (100 ppm) and TA (100 ppm), $CaCl_2$ (10 mM) and NaCl (10 mM); draw solution (5 M NaCl); AL-FS orientation; 1.5 cm/s CFV.***

Obtained results show that during the 1st filtration run, the water flux gradually decreased to 80% and 70% during the first 6 and 12 hours, respectively. After applying the surface wash, the flux was recovered to 100%. After 3 hours of the 2nd filtration run, the water flux decreased to 70%. A further reduction in water flux was up to 57%. Unlike the 1st run, a rapid decrease in flow occurred during the 2nd run. It is likely that the rapid drop in flow occurred as a result of membrane fouling, that was poorly recovered due to surface rinsing.

Figure 3-24 illustrates the effect of modified membrane to recover from surface rinsing after 1st run of fouling experiments.

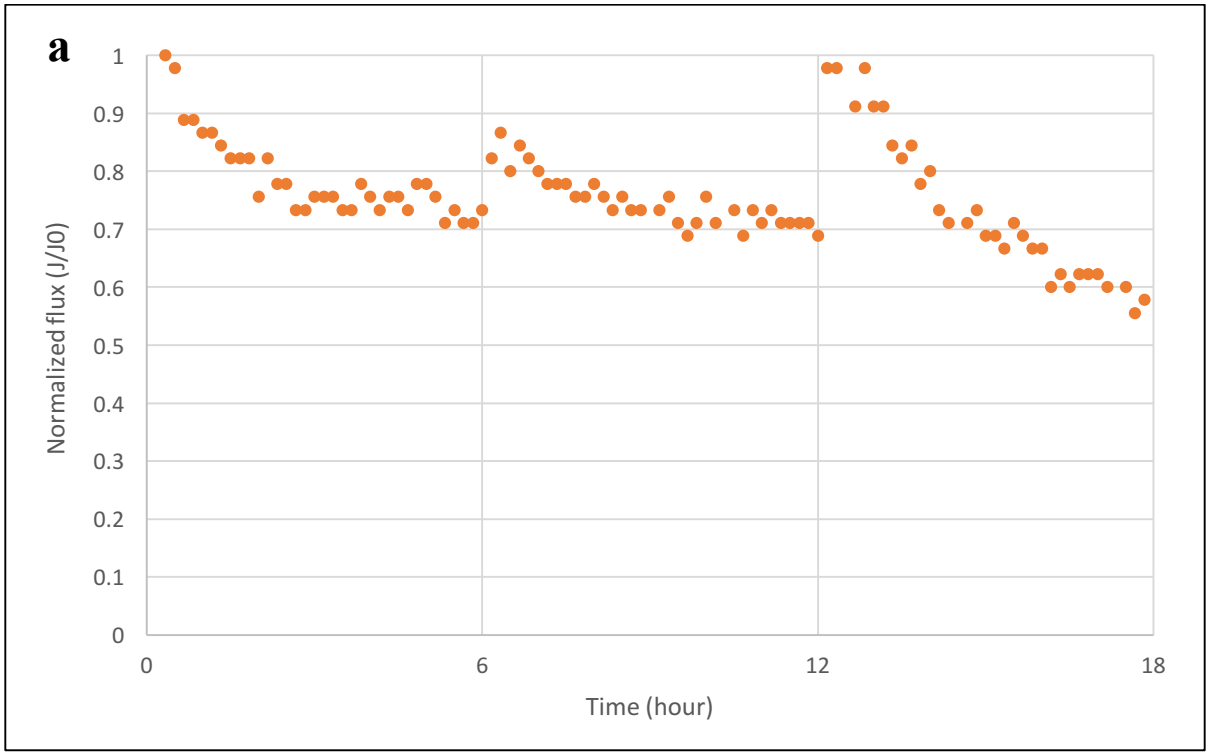

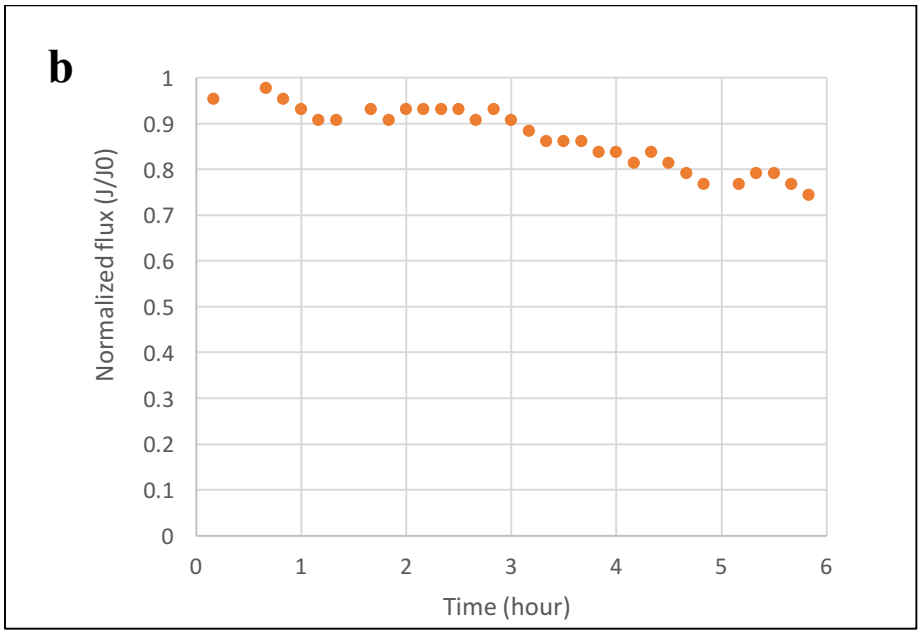


***Figure 3-24. Normalized water flux of fouling experiment for modified membrane: a) before surface rinsing and b) after surface rinsing. Experimental conditions for fouling experiments: feed solution (mixture of ALG (100 ppm), BSA (100 ppm) and TA (100 ppm), $CaCl_2$ (10 mM) and NaCl (10 mM); draw solution (5 M NaCl); AL-FS orientation; 1.5 cm/s CFV***

By comparing flux profiles of the 1st run of fouling experiments for pristine and modified membranes, it can be observed that membrane underwent to modification was able to restore flux value after each 6 hour fouling session. Figure 3-24a shows that after the first 6 hours, membrane flux dropped by 29%, but after it restored by 13% flux and again declined to 68% of the initial flux during next 6 hours. After 12 hours of fouling modified membrane again was able to recover to initial conditions, but during next 6 hours has lost permeability level to 58%. Further, as for pristine membrane surface rinsing was performed and fouling experiment repeated for same membrane, which showed 26% flux steady

flux drop during 6 hours. It should be noted that in case of pristine membrane (3-23), the flux after the 2nd run reduced to 57% (43% flux loss).

### 3.5.2 – Osmotic backwash

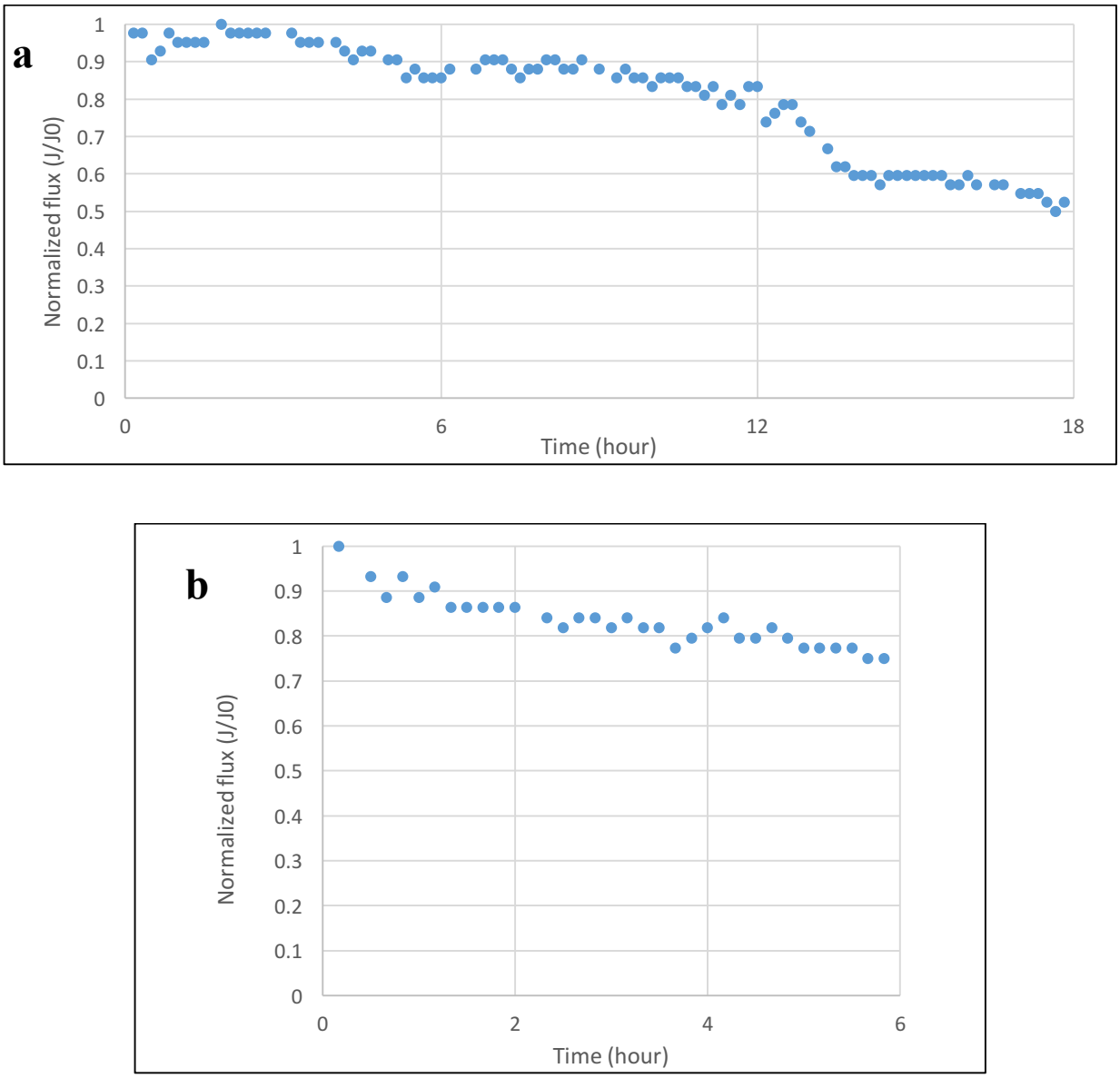


***Figure 3-25. Normalized water flux of fouling experiment for pristine membrane: a) before osmotic backwash and b) after osmotic backwash. Experimental conditions for fouling experiments: feed solution (mixture of ALG (100 ppm), BSA (100 ppm) and TA (100 ppm), $CaCl_2$ (10 mM) and NaCl (10 mM); draw solution (5 M NaCl); AL-FS orientation; 1.5 cm/s CFV***

Figure 3-25 shows the flow restoration and performance of the primary membrane after osmotic backwash. It can be seen that after the membrane was fouled (Figure 3-25a) after 18 hours, the membrane, as in the previous cases, could fully recover after osmotic backwash. However, compared to rinsing the surface (flux loss of 43%), the osmotic backwash effect is more beneficial for a pristine membrane, which has reduced its flow to 75%. Thus, cleaning the pores and membrane surfaces with an osmotic backwash has a good effect on the pristine membrane compared to rinsing the surface.

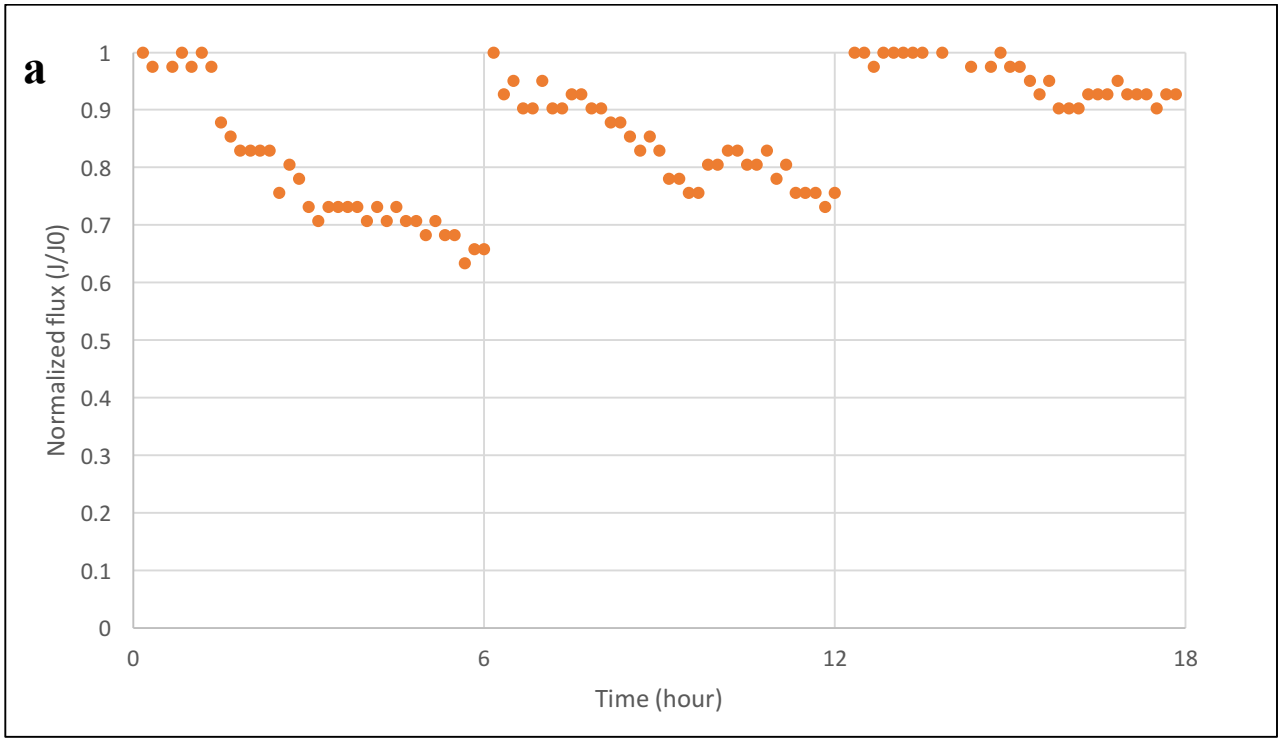

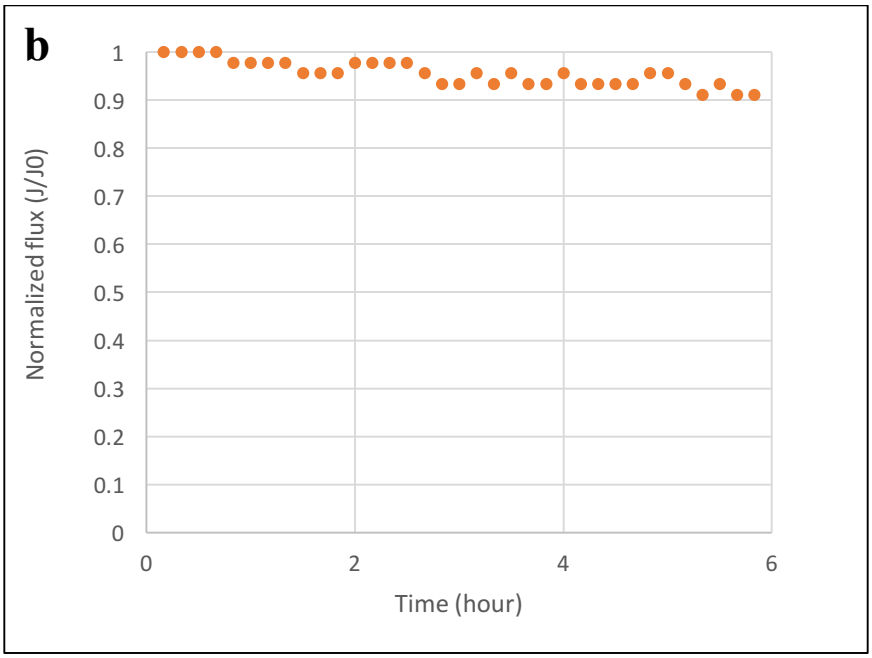


***Figure 3-26. Normalized water flux of fouling experiment for modified membrane: a) before osmotic backwash and b) after osmotic backwash. Experimental conditions for fouling experiments: feed solution (mixture of ALG (100 ppm), BSA (100 ppm) and TA (100 ppm), $CaCl_2$ (10 mM) and NaCl (10 mM); draw solution (5 M NaCl); AL-FS orientation; 1.5 cm/s***

On the basis of Figure 3-26a, it can be seen that after 6-hour fouling of the 1st run for the modified membrane, the flow dropped to 60%, and after relaxation the flux level restored to the starting point. The same behavior was repeated after 12 hours of the 1st run, when the flow fell from 100% to 75% and from 100% to 92% (Fig. 3-26a). After the osmotic backwash, the membrane was again fouled for 6 hours, after which only 9% flux loss was observed (Figure 3-26b). Looking at the graphs, it can be seen that the pristine membrane lost 25% of the flow, while the modified membrane lost only 9% of the initial flow. Thus, the results obtained indicate that the modified membrane has better performance after the osmotic backwash.

### 3.5.3 – CFV magnification

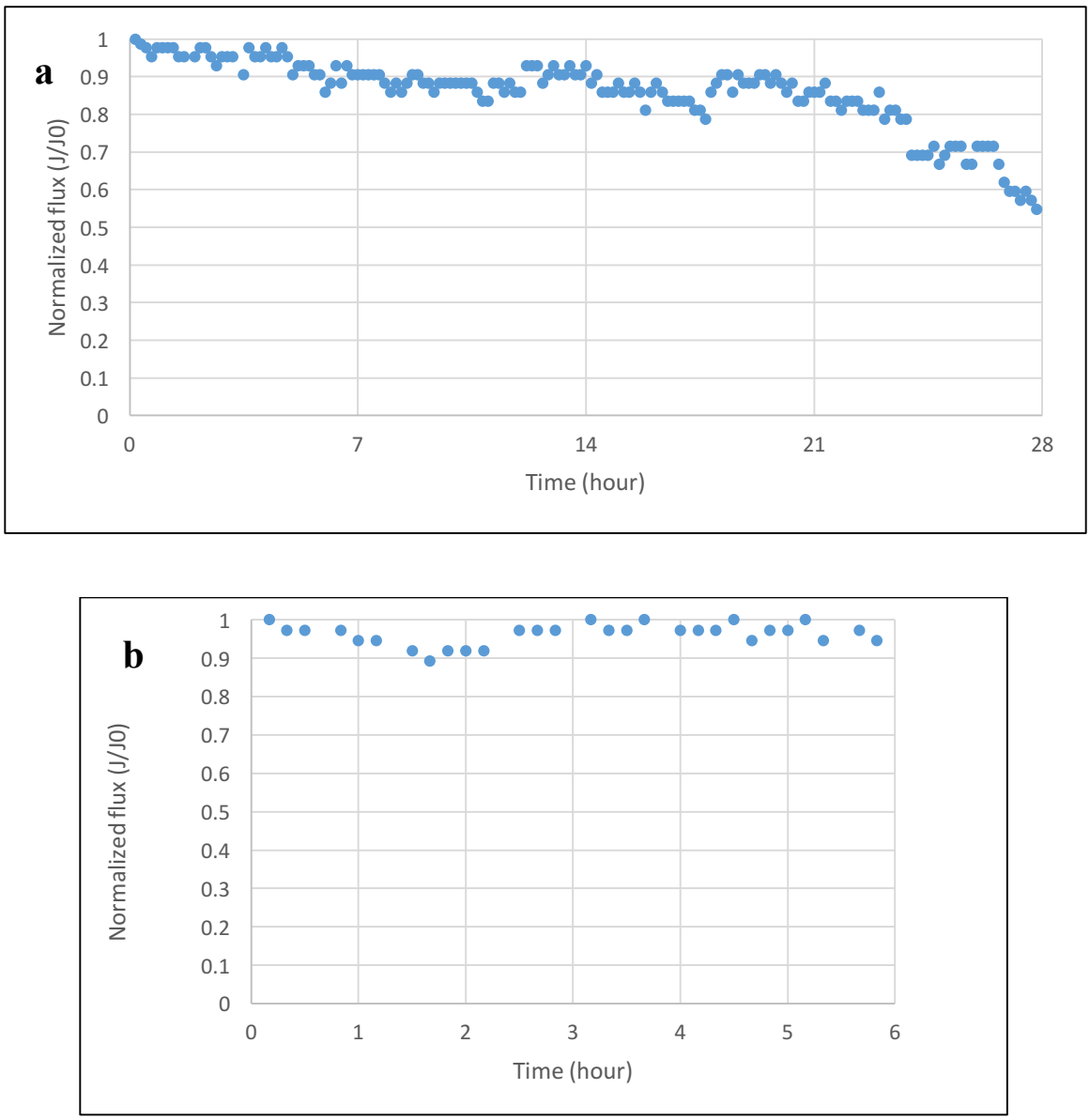


***Figure 3-27. Normalized water flux of fouling experiment for pristine membrane: a) before CFV magnification and b) CFV magnification. Experimental conditions for fouling experiments: feed solution (mixture of ALG (100 ppm), BSA (100 ppm) and TA (100 ppm), $CaCl_2$ (10 mM) and NaCl (10 mM); draw solution (5 M NaCl); AL-FS orientation; 1.5 cm/s CFV for the 1st run, 6 cm/s CFV for the 2nd run***

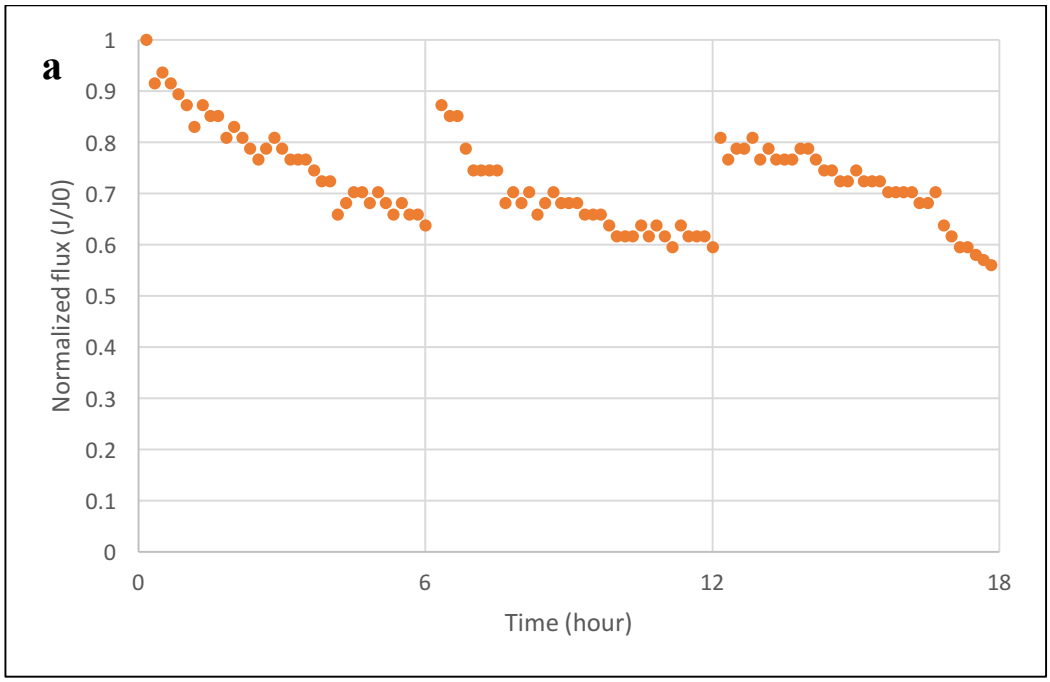


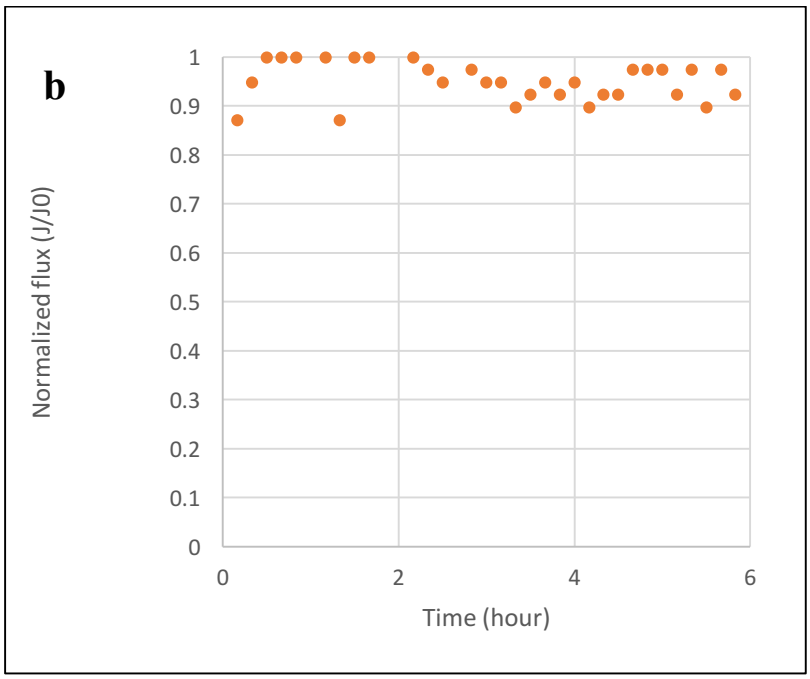


***Figure 3-28. Normalized water flux of fouling experiment for modified membrane: a) before CFV magnification and b) CFV magnification. Experimental conditions for fouling experiments: feed solution (mixture of ALG (100 ppm), BSA (100 ppm) and TA (100 ppm), $CaCl_2$ (10 mM) and NaCl (10 mM); draw solution (5 M NaCl); AL-FS orientation; 1.5 cm/s CFV for the 1st run, 6 cm/s CFV for the 2nd run***

The figures 3-27 and 3-28 provide results collected from CFV magnification after both pristine and modified membranes got fouled. In general, it can be seen that fouled membranes produced much higher and stable water flux when velocity of flow quadrupled. The pristine membrane piece in this experiment was able to get fouled only after 28 hours of fouling experiments, while modified membrane fouled after 18 hours. However, if pristine membrane loses flux levels steadily, the modified membrane as in previous cases after each 6-hour experiment could restore flux values. This shows, that membranes with silver nanoparticles are able to recover from foulants but fouling happens at a much higher rate.

To observe how Ag-NPs affecting membrane performance after cleaning, each membrane was subjected to an experiment with fouling to achieve a 50% flux loss. The results show that immobilization of silver nanoparticles on a membrane gives a different behavior than an pristine membrane. Figure 3-24 (surface rinsing for modified membrane), figure 3-26 (osmotic backwash for modified membrane), and figure 3-28 (CFV magnification for modified membrane) show that the modified membranes acquired the ability to regenerate the flux after every 6 hours of fouling, which is not characteristic of the primary membrane, which gradually loses the flux. This can be explained by the ability of silver nanoparticles to

decompose organic macromolecules upon their contact [77]. In the case of a pristine membrane, contaminated organic matter sticks to the surface and inside the pores, but in the case of a modified membrane, the ability of the membrane to decompose organic contamination makes it possible to restore its permeable ability each time.

Furthermore, after the membrane was contaminated, a special cleaning procedure was carried out. After the surface of membrane was washed with deionized water (surface rinsing), the flux of pristine and modified membranes was restored to 100%. However, after the 2nd cycle of contamination, the primary and modified membranes lost their flux by 43% and 26%, respectively. Better effect was observed when the membranes were subjected to osmotic backwashing, which showed a 25% and 9% decrease in flux for pure and modified membranes, respectively. This is due to the difference in the methods used. If in the case of rinsing only the membrane surface was cleaned, in case of osmotic backwashing the pores and surface were cleaned. Thus, silver nanoparticles contributed to the fall of up to 91% of the initial flux for the modified membrane after osmotic backwash and the 2nd run of fouling experiment.

The increase in CFV from 1.5 cm s to 6 cm/s for the 2nd run of fouling experiments shows that the loss of flux compared with other cases has a positive

reflection in the values of water flux for both the primary and modified membranes. This means that the high flow rate of water stream prevents organic molecules from forming an organic gel layer on the membrane surface, even if the membrane was initially contaminated with foulants. Thus, this shows that among all the listed cleaning methods for pristine and modified membranes CFV magnification has the most beneficial impact in terms of flux loss.

# Chapter 4 – Conclusion

This work describes the implementation of innovative, effective and optimal way of modification of aquaporin membranes with silver nanoparticles. The TFC FO membrane with aquaporin underwent modification and was characterized for analysis on the change in properties. The performance of membranes was further studied by conducting filtration and cleaning experiments. In comparison with non-modified membranes, silver modified aquaporin membrane demonstrates significant results in prevention of biofouling and retaining of organic compounds, and causes improvement of general properties and quality of the membrane itself. Obtained results show that attachment of silver nanoparticles not only benefit water flux levels, the long term experiment has revealed ability of modified

membranes to recover from fouling. The fouling experiments demonstrated that modified membranes have less fouling loss and cleaning procedures (surface rinsing, osmotic backwash and CFV magnification) can positively influence further filtration.

This work is the result of combination of several studies and application of previous methods and experiments on exploration and further modification of membranes in order to find the most optimal way of avoiding organic and biofouling. Method used for modification of aquaporin membrane demonstrates simple, relatively inexpensive and accurate way of applying silver nanoparticles. Findings of this study demonstrate one possible way to improve and make water treatment techniques more available. After the modification of membrane following conclusions were achieved:

-successful attachment of Ag-NPs;

- antimicrobial property against biofilm formation;

- maintaining physical and chemical integrity;

- the ability of aquaporin channels to permeate water;

- the ability to effectively filter water after cleaning.

# References

[1] Lutchmiah,K., Verliefde, A.R.D, Roest, K., Rietveld, L.C, Cornelissenk, E.R., 2014, “Forward osmosis for application in wastewater treatment: A review.” Water Research. 58, 179-197..

[2] Van Der Bruggen, B., Vandecasteele, C., Doyen, W., Leysen, R., 2003, “A Review of Pressure-Driven Membrane Processes in Wastewater Treatment and Drinking Water Production.” Env. progress. 22, 46-56. doi:10.1002/ep.670220116.

[3] Hendricks, D., 2011, “Fundamentals Of Water Treatment Unit Processes.” Boca Raton: CRC Press; 543-544.

[4] Pendergast, M.T. Hoek, E., 2011, “A review of water treatment membrane nanotechnologies.” Energy Environ. Sci.4, 1946-1971. doi: 10.1039/C0EE00541J.

[5] Van Der Bruggen, B., Vandecasteele, C., Doyen, W., Leysen, R.,2003, “A Review of Pressure-Driven Membrane Processes in Wastewater Treatment and Drinking Water” Production. Env. progress. 22, 46-56. doi:10.1002/ep.670220116.

[6] Pinnau, I.; Freeman, B. D., 2000, “ In Formation and Modification of Polymeric Membranes”, ACS Symposium Series 744; American Chemical Society: Washington D.C., pp 1-22.

[7] Cheryan, M., 2010, “Ultrafiltration And Microfiltration”. Boca Raton: CRC Press; 129-139.

[8] Hendricks, D., 2011, “Fundamentals Of Water Treatment Unit Processes.” Boca Raton: CRC Press; 543-544.

[9] De Meis, D., 2017, “Overview on porous inorganic membranes for gas separation.”, doi: 10.13140/RG.2.2.35571.53287.

[10] Radcliff, R.Z.A., 2004, “Application of Membrane Technology to the Production of Drinking Water,” Water Conditioning & Purification, p. 23-25.

[11] Pinnau, I.; Freeman, B. D., 2000, “ In Formation and Modification of Polymeric Membranes”, ACS Symposium Series 744; American Chemical Society: Washington D.C., pp 1-22.

[12] Baker, R. W., 2004, “Membrane Technology and Applications”, 2nd ed.; John Wiley & Sons, Ltd.: Chichester.

[13] Nunes, S. P., Peinemann, K. V., 2001, “Membrane Technology in the Chemical Industry”, WileyVCH: Weinheim.

[14] Ulbricht, M.,2006, “ Advanced functional polymer membranes,” Polymer, 47: p. 2217-2262.

[15] Beier, S.P.,2013, “Pressure Driven Membrane Processes - 2nd edition”, BookBoon.

[16] Tewari, P.K, 2017, "Nanocomposite Membrane Technology: Fundamentals and Applications", ISBN 9781138749122 - CAT# K32716, CRCPress.

[17] Shon, H.K.,2013, “Nanofiltration for water and wastewater treatment – a mini review”, Drinking Water Engineering and Science, 6(1): p. 47-53.

[18] Faria, A.F., Liu, C., Xie, M., Perreault, Nghiem, F. L. D., Ma, J., Elimelech, M., , "Thin-film composite forward osmosis membranes functionalized with graphene oxide–silver nanocomposites for biofouling control," Journal of Membrane Science, vol. 525, pp. 146–156.

[19] Greenlee, L.F., 2009, " Reverse osmosis desalination: Water sources, technology, and today's challenges", Water Research, 43(9): p. 2317-2348.

[20] Pressdee, J.R., 2006, "Integration of Membrane Filtration Into Water Treatment Systems," Awwa Research Foundation/ American Water Works Association/ IWA Pub.

[21] Valladares Linares, R. "Recent developments in forward osmosis processes."

[22] Zhang, M., Shan, J., Tang, C.,2014, "Gypsum scaling during forward osmosis process—a direct microscopic observation study." *Desalination and Water Treatment*. 57(8):3317-3327. doi:10.1080/19443994.2014.985727.

[23] Chun, Y., Mulcahy, D., Zou, L., Kim, I.S, "A Short Review of Membrane Fouling in Forward Osmosis Processes".

[24] DOI: 10.1016/j.desal.2017.11.041

[25] Tang, C., Zhao, Y., Wang, R., Hélix-Nielsen, C., Fane, A., 2017, "Desalination by biomimetic aquaporin membranes: Review of status and prospects".

[26] Giwa, A., Hasan, S., Yousuf, A., Chakraborty, S., Johnson, D., Hilal, N., 2017, "Biomimetic membranes: A critical review of recent progress", Desalination, vol. 420, pp. 403-424.

[27] Zhao, Y., Qiu, C., Li, X., Vararattanavech, A., Shen, W., Torres, J., Hélix-Nielsen, C., Wang, R., Hu, X., Fane, A.G., Tang, C.Y., 2012, "Synthesis of robust and high-performance aquaporin-based biomimetic membranes by interfacial polymerization-membrane preparation and RO performance characterization", Journal of Membrane Science, vol. 423–424, pp.422–428.

[28] Kumar, R. and Ismail, A.F., 2015, "Fouling control on microfiltration/ultrafiltration membranes: Effects of morphology, hydrophilicity, and charge." Journal of Applied Polymer Science, 132(21): p. n/a-n/a.

[29] Abdelrasoul, A., Doan, H., Lohi,A., 2013, "Fouling in Membrane Filtration and Remediation Methods, in Mass Transfer - Advances in Sustainable Energy and Environment Oriented Numerical Modeling", InTech: Rijeka. p. Ch. 08.

[30] Li, Z., Valladares Linares, R., Bucs, S., Fortunato, L., Hélix-Nielsen, C., Vrouwenvelder, J., Ghaffour, N., Leiknes, T., Amy, G., 2017. "Aquaporin based biomimetic membrane in forward osmosis: Chemical cleaning resistance and practical operation", Desalination, vol. 420, pp. 208-215.

[31] Wang, X., Zhao,Y., Yuan, B., Wang, Z., Li, X., Ren, Y., 2016, "Comparison of biofouling mechanisms between cellulose triacetate (CTA) and thin-film composite (TFC) polyamide forward osmosis membranes in osmotic membrane bioreactors," Bioresource Technology, vol. 202, pp. 50-58.

[32] Zhang, Q., Jie, Y., Loong, W., Zhang, J., Fane, A., Kjelleberg, S., Rice, S., McDougald, D., 2014, "Characterization of biofouling in a lab-scale forward osmosis membrane bioreactor (FOMBR)", Water Research, vol. 58, pp. 141-151.

[33] Morones, J., Elechiguerra, J., Camacho, A., Holt, K., Kouri, J., Ramírez, J., Yacaman, M.,2005, "The bactericidal effect of silver nanoparticles", Nanotechnology, vol. 16, no. 10, pp. 2346-2353.

[34] Teow, Y.H., Mohammad, A. W., 2018, "New generations nanomaterials for water desalination: A review", Desalination, 451, p.2-17. doi: https://doi.org/10.1016/j.desal.2017.11.041

[35] Flemming, H.C., 1997, "Biofouling—the Achilles heel of membrane processes." Desalination, 113(2): p. 215-225.

[36] Arkhangelsky, E., Wicaksana, F., Chou, S., Al-Rabiah, A., Al-Zahrani, S., Wang, R., 2012, "Effects of scaling and cleaning on the performance of forward osmosis hollow fiber membranes," *Journal of Membrane Science*.415-416:101-108. doi:10.1016/j.memsci.2012.04.041.

[37] Hadrup, N., Lam, R., H., n.d., "Oral toxicity of silver ions, silver nanoparticles and colloidal silver – A review," doi.org/10.1016/j.yrtph.2013.11.002.

[38] Yang, Y., Chen, Q., Wall, J.D., Hu, Z., 2012, "Potential nanosilver impact on anaerobic digestion at moderate silver concentrations," Water Research, vol. 46, no. 4, pp. 1176–1184.

[39] Bogler, A., Lin, S., Bar-Zeev, E., 2017, "Biofouling of membrane distillation, forward osmosis and pressure retarded osmosis: Principles, impacts and future directions", Journal of Membrane Science, vol. 542, pp. 378-398.

[40] Morones, J., Elechiguerra, J., Camacho, A., Holt, K., Kouri, J., Ramírez, J., Yacaman, M., 2005, "The bactericidal effect of silver nanoparticles", Nanotechnology, vol. 16, no. 10, pp. 2346-2353, 2005.

[41] Dolina, J., Dlask,O., Lederer, T., Dvořák, L., 2015,"Mitigation of membrane biofouling through surface modification with different forms of nanosilver", Chemical Engineering Journal, vol. 275, pp. 125-133.

[42] KeunSon, W., HoYouk, J., HoPark, W., “Antimicrobial cellulose acetate nanofibers containing silver nanoparticles.” doi.org/10.1016/j.carbpol.2006.01.037

[43] Niemietz, M.C., Tyerman, D.T., 2002, “New potent inhibitors of aquaporins: silver and gold compounds inhibit aquaporins of plant and human origin.”

[44] Kalafatakis1, S., Braekevelt, S., 2018, “Application of forward osmosis technology in crude glycerol.”

[45] Dadosh T., 2009, “:Synthesis of uniform silver nanoparticles with a controllable size.”, Materials Letters. 63, 2236-2238. doi:10.1016/j.matlet.2009.07.042.

[46] Piella, J., Bastus, N.G., Puntes, V., 2016, “Size-Controlled Synthesis of Sub-10-nanometer Citrate-Stabilized Gold Nanoparticles and Related Optical Properties.”, Chemistry of Materials. 28, 1066-1075. doi:10.1021/acs.chemmater.5b04406.

[47] Soroush, A, Ma., W., Silvino, Y., Rahaman, M., 2015, “Surface modification of thin film composite forward osmosis membrane by silver-decorated graphene-oxide nanosheets,” Environmental Science: Nano. 395-405. DOI: 10.1039/c5en00086f.

[48] Yin, J., Yang, Y., Hu, Z., Deng, B., 2013, "Attachment of silver nanoparticles (AgNPs) onto thin-film composite (TFC) membranes through

covalent bonding to reduce membrane biofouling," Journal of Membrane Science, vol. 441, pp. 73-82, 2013.

[49] Prakash, R.A. , Joshi, S., Trivedi, J., Devmurari, C., Shah, V., 2003, "Structure–performance correlation of polyamide thin film composite membranes: effect of coating conditions on film formation,", *Journal of Membrane Science*. 211(1):13-24. doi:10.1016/s0376-7388(02)00305-8.

[50] Li, X., Zhang, C., Zhang, S., Li, J., He, B., Cui, Z., Preparation and characterization of positively charged polyamide composite nanofiltration hollow fiber membrane for lithium and magnesium separation. *Desalination*. 2015; 369:26-36. doi:10.1016/j.desal.2015.04.027.

[51] Tang, C., Kwon, Y., Leckie, J., 2009, "Effect of membrane chemistry and coating layer on physiochemical properties of thin film composite polyamide RO and NF membranes," *Desalination*, 242(1-3):149-167.doi:10.1016/j.desal.2008.04.003.

[52] Jia, Q., Xu, Y., Shen, J., Yang, H., Zhou, L., 2015, "Effects of hydrophilic solvent and oxidation resistance post surface treatment on molecular structure and forward osmosis performance of polyamide thin-film composite (TFC) membranes,"*Applied Surface Science*. 356:1105-1116. doi:10.1016/j.apsusc.2015.08.129.

[53] Hey, T., Zarebska, A., Bajraktari, N., (2016), "Influences of mechanical pretreatment on the non-biological treatment of municipal wastewater by forward osmosis," *Environmental Technology*. 38(18):2295-2304. doi:10.1080/09593330.2016.1256440.

[54] Jia, Q., Han, H., Wang, L., Liu, B., Yang, H., Shen, J., 2014, "Effects of CTAC micelles on the molecular structures and separation performance of thin-film composite (TFC) membranes in forward osmosis processes", *Desalination*. 340:30-41. doi:10.1016/j.desal.2014.02.017.

[55] Jia, Q., Han, H., Wang, L., Liu, B., Yang, H., Shen, J., 2014, "Effects of CTAC micelles on the molecular structures and separation performance of thin-film composite (TFC) membranes in forward osmosis processes,", *Desalination*, 340:30-41. doi:10.1016/j.desal.2014.02.017.

[56] Wroblewska, A., Zych, A., 2015, "Thiyagarajan S et al. Towards sugar-derived polyamides as environmentally friendly materials.", *Polymer Chemistry*. 6(22):4133-4143. doi:10.1039/c5py00521c.

[57] Sridhar, S., Smitha, B., Mayor, S., Prathab, B., Aminabhavi, T., 2007, "Gas permeation properties of polyamide membrane prepared by interfacial polymerization," *Journal of Materials Science*. 42(22):9392-9401. doi:10.1007/s10853-007-1813-5.

[58] Singh, P., Joshi, S., Trivedi, J., Devmurari, C., Rao, A., Ghosh, P., 2005, "Probing the structural variations of thin film composite RO membranes obtained by coating polyamide over polysulfone membranes of different pore dimensions," *Journal of Membrane Science*. 278(1-2):19-25. doi:10.1016/j.memsci.2005.10.039.

[59] Socrates, G., 2000, "*Infrared Characteristic Group Frequencies*." New York: Wiley, 145-148.

[60] Zhang, M., Hou, D., She, Q., Tang, C., 2013, "Gypsum scaling in pressure retarded osmosis: Experiments, mechanisms and implications." *Water Res*. 2014;48:387-395. doi:10.1016/j.watres.2013.09.051.

[61] Jin, X., Tang, C., Gu, Y., She, Q., Qi, S., 2011, "Boric Acid Permeation in Forward Osmosis Membrane Processes: Modeling, Experiments, and Implications." *Environ Sci Technol*. 45(6):2323-2330. doi:10.1021/es103771a.

[62] Teow, Y.H., Mohammad, A. W., 2018, "New generations nanomaterials for water desalination: A review", Desalination, 451, p.2-17. doi: https://doi.org/10.1016/j.desal.2017.11.041

[63] Oo, M., Ong, S., 2010, "Implication of zeta potential at different salinities on boron removal by RO membranes," *Journal of Membrane Science*. 352(1-2):1- 6. doi:10.1016/j.memsci.2010.01.030.

[64] Wang, L., Fang, M., Liu, J., He, J., Deng, L., Li, J., & Lei, J., 2015, "The influence of dispersed phases on polyamide/ZIF-8 nanofiltration membranes for dye removal from water", RSC Advances, 5(63), 50942–50954. doi:10.1039/c5ra06185g.

[65] Ali, M. E. A., Hassan, F. M., & Feng, X., 2016, "Improving the performance of TFC membranes via chelation and surface reaction: applications in water desalination," Journal of Materials Chemistry A, 4(17), 6620–6629. doi:10.1039/c6ta01460g

[66] Cosgrove, T., 2005, "Colloid science: Principles, methods and applications," Blackwell Publishing: UK.

[67] Hadrup, N., Lam, R., H., n.d., "Oral toxicity of silver ions, silver nanoparticles and colloidal silver – A review," doi.org/10.1016/j.yrtph.2013.11.002.

[68] Sau, T. K., Pal, A., Jana, N. R., Wang, Z. L., & Pal, T., 2001, "Size controlled synthesis of gold nanoparticles using photochemically prepared seed particles," Journal of Nanoparticle Research, 3(4), 257–261. doi:10.1023/a:1017567225071

[69] Tiraferri, A., Kang, Y., Giannelis, E., Elimelech, M., 2012, "Highly Hydrophilic Thin-Film Composite Forward Osmosis Membranes Functionalized with Surface-Tailored Nanoparticles." *ACS Appl Mater Interfaces*. 4(9):5044-5053. doi:10.1021/am301532g.

[70] Yang, Z., Wu, Y., Guo, H., Lin, C., Zhou, Y., Cao, B., Zhu, B., Shih, K., Tang, C. Y., 2017, "A novel thin-film nano-templated composite membrane with in situ silver nanoparticles loading: Separation performance enhancement and implications". Journal of Membrane Science, 544, 351-358.

[71] Soroush, A., Ma, W., Silvino, Y., Rahaman, M., 2015, "Surface modification of thin film composite forward osmosis membrane by silver-decorated graphene-oxide nanosheets." Environmental Science: Nano. 395-405. DOI: 10.1039/c5en00086f.

[72] Huynh, A.K., McCaffery, J.M., and Kai, .L.C., 2014, Heteroaggregation Reduces Antimicrobial Activity of Silver Nanoparticles: Evidence for Nanoparticle–Cell Proximity Effects.

[73] Xu, F., Weng, B., Materon, L. A., Kuang, A., Trujillo, J. A., & Lozano, K., 2016, "Fabrication of cellulose fine fiber based membranes embedded with silver nanoparticles via Forcespinning, "Journal of Polymer Engineering, 36(3). doi:10.1515/polyeng-2015-0092

[74] Russell, A.D, Hugo, W.B., 1994, "Antimicrobial activity and action of silver," Prog. Med. Chem., 31, 351–370.

[75] Choi, O., Deng, K.K., Kim, N.J., Ross, L., Surampalli, R.Y., Hu,Z., 2008, "The inhibitory effects of silver nanoparticles, silver ions, and silver chloride colloids on microbial growth," Water Res. 42, 3066–3074.

[76] Lok, C.N. Ho, C.M., Chen, R., He, Q.Y., Yu, W.Y., Sun, H., Tam, P.K.H., Chiu, J.F. , Che, C. M., 2006, "Proteomic analysis of the mode of antibacterial action of silver nanoparticles," J. Proteome Res. 5, 916–924.

[77] Nguyen, A., Zou, L., & Priest, C., 2014, "Evaluating the antifouling effects of silver nanoparticles regenerated by TiO2 on forward osmosis membrane," Journal of Membrane Science, 454, 264–271. doi:10.1016/j.memsci.2013.12.024